Draft version November 9, 2022
Typeset using LaTeX **modern** style in AASTeX631

Apophis Specific Action Team Report

Jessie L. Dotson [1,*] Marina Brozovic,[2] Steven Chesley [2] Stephanie Jarmak,[3,*] Nicholas Moskovitz [4] Andrew Rivkin [5] Paul Sánchez [6] Damya Souami [7] and Timothy Titus [8,*]

[1] *NASA Ames Research Center*
[2] *Jet Propulsion Laboratory, California Institute of Technology*
[3] *Southwest Research Institute*
[4] *Lowell Observatory*
[5] *John Hopkins Applied Physics Laboratory*
[6] *University of Colorado, Boulder*
[7] *Observatoire de la Côte d'Azur, Nice, France*
[8] *US Geological Survey*

1. EXECUTIVE SUMMARY

This report about Asteroid (99942) Apophis's Earth close approach on April 13, 2029 was generated by a Specific Action Team (SAT) formed by the Small Body Assessment Group (SBAG) at the resquest of NASA's Planetary Science Division (PSD). The SAT assessed the current predictions for the effects that may occur due to the close encounter, evaluated observing capabilities, and identified possible investigations then sorted them into priority categories. In addition, the SAT evaluated whether or not a spacecraft sent to Apophis could increase the risk of a future Earth impact. The top level conclusions of the SAT are listed below.

Effects of the Encounter: While the Apophis Earth close approach has been modeled by several authors, the quantitative details of the predicted effects vary from model to model and are, in general, sensitive to uncertainties about Apophis's shape, internal structure, and rotational state during the close approach. As a result it is not currently possible to definitively quantify the likely outcome of the close approach. Nonetheless, there were sufficient trends in the existing predictions that the SAT could identify likely opportunities and assess the scientific impact of non-detections. The asteroid's orbit will definitely change and its spin state will most likely undergo a significant change. Apophis's surface may experience localized areas of resurfacing. The asteroid is less likely to experience changes in shape. There are a couple of intriguing possible effects which were not assessed due to the scarcity of adequate models, including the response of

[*] member of Small Bodies Assessment Group Steering Committee

a contact binary internal configuration to tidal stresses and electrostatic lofting in the near-Earth environment.

Observational Capabilities: A wide variety of observational capabilities will have rare opportunities during the close encounter. In some cases, this is due to the prospect of observing the possible effects of the close encounter and in some cases it is due to the nearness and/or brightness of the asteroid during the close encounter. Ground-based radar, ground-based optical light curve photometry, and optical-near IR multi-band high resolution imaging from a spacecraft could be significant contributors to high impact investigations. The science output from the encounter would benefit from practice campaigns, coordination, and timely data sharing. Additionally, the design of spacecraft visiting during the close encounter should include a plan for robust operations during radar observations. Finally, the close approach could also provide an opportunity to demonstrate the efficacy of several observing methods which are not at present commonly used for small bodies research such as long wavelength radar, polarimetry, and speckle photometry.

Top Priority Investigations: The SAT identified two top priority investigations. The close encounter provides a rare opportunity to directly observe a geophysical process, resurfacing due to tidal effects, in real time rather than just inferring its effects. This investigation could be performed by a multi-band high resolution optical-near IR imager on one or more spacecraft near the asteroid before and after the close approach. (Observations during the close approach are desireable, but not essential to this investigation.) The outcome of this investigation (including a null result) would provide unprecedented detail about a geophysical process, contribute to our understanding of how surfaces of asteroids evolve, and enable estimates of regolith cohesion. The study of geophysical processes and the evolution of the surfaces of small bodies is integral to planetary science. Cohesive strength of regolith is an important factor in how asteroid surfaces respond to disturbances, whether natural or caused by humans, and is therefore of interest to both planetary science and planetary defense.

Another top priority investigation would yield information about the interior mass distribution and strength of Apophis, topics of interest to both planetary science and planetary defense. The interior structure of an asteroid carries the imprint of its collisional and accretion history and is a source of significant uncertainty about how an asteroid would react during atmospheric entry or respond to a mitigation attempt. The non-principal axis rotation of Apophis enables insight about the asteroid's interior since a comparison of dynamical and shape-based moment of inertia ratios can provide insight about the mass distribution. Furthermore, models of the spin state change will provide additional constraints about how uniform (or non-uniform) the mass distribution

is within the asteroid as well as constraints on the strength of the body. Any change in moment of inertia ratios pre- and post- flyby, signaling the shape change, will be monitored as well. Ground based radar and optical photometry can provide the required pre- and post- encounter spin state information. Shape models derived from ground based radar will be sufficient for this investigation.

Hazard Assessment for Spacecraft Contacts with Apophis: The SAT assessed the effects on potential Earth impacts over the next century due to a spacecraft which interacts with Apophis anytime during the decade centered on the Earth close approach (April 2024 - April 2033). Two representative values of ΔV were considered. One, $\Delta V_{\rm KI} = 1$ mm/s, is representative of a kinetic impactor mission and the other, $\Delta V_{\rm Sci} = 7$ μm/s, is a plausible upper limit for a science mission. The slight deflection associated with the science investigation case will not cause Apophis to impact Earth within 100 years from present. However, the situation is more subtle for the larger deflections that may be associated with a kinetic energy deflection demonstration. We find that such deflections are assuredly safe only if applied after the Apophis close encounter with Earth in April 2029. Deflections of such magnitude applied before April 2029 will greatly increase the spread of possible trajectories of Apophis after the 2029 encounter and thus require a detailed analysis (beyond the scope of this report) that takes into account the direction and magnitude of planned deflection and fully accounts for nonlinearities in the mapping from the deflection epoch to subsequent encounters.

2. INTRODUCTION

Asteroid (99942) Apophis's Earth close approach on April 13, 2029 will be an extremely rare event. Passages of an object this large or larger, this deep or deeper through Earth's gravitational tidal field, are estimated to occur at a mean interval on the order of a thousand years. In order to assess and evaluate the scientific opportunities afforded by this close approach, NASA's Planetary Science Division requested that the Small Body Assessment Group convene a Specific Action Team. The primary tasks are as follows: (A complete terms of reference are included in the Appendix.)

1. Identify and quantify the detectable effects on Apophis expected from the Earth encounter and identify the measurements and instrumental sensitivities needed to detect them and determine their magnitudes.

2. Assess and Prioritize the importance to planetary science and planetary defense of detecting and measuring each of these effects, as well as the value of non-detections (upper limits).

3. Categorize these effects according to *(a)* detectable using Earth-based assets, *(b)* detectable using a spacecraft arriving only after Earth close approach, and *(c)* detectable using a spacecraft arriving before Earth close approach.

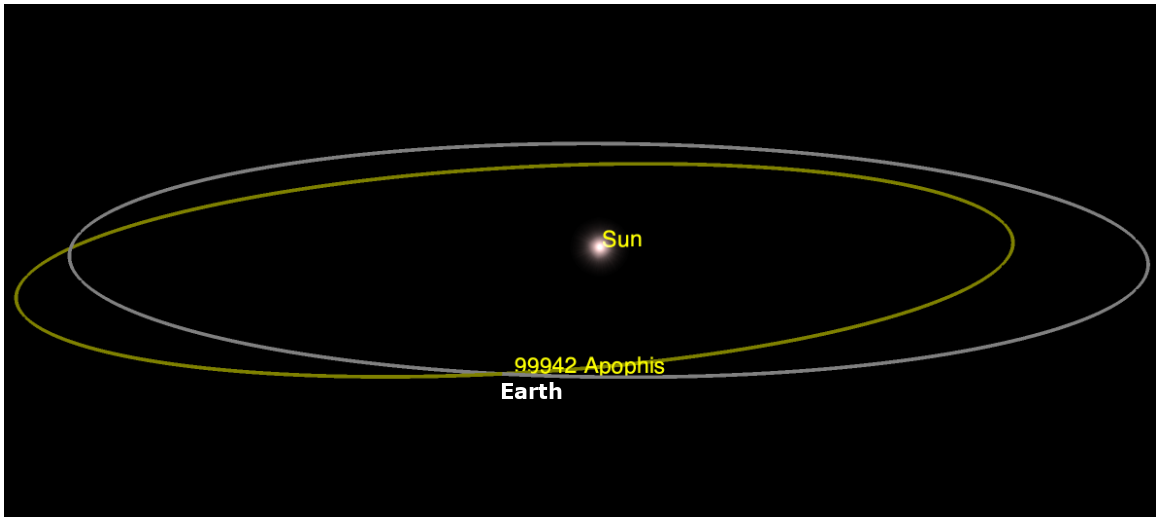

Figure 1. Apophis heliocentric orbital position on April 13, 2029. The closest approach occurs at 21:46 UTC at 0.1 lunar distance. Figure generated with Cosmographia software using SPICE (Acton et al. 2018).

4. Quantitatively assess the possibility that spacecraft sent to Apophis could increase the risk of a future Earth impact.

The report is structured as follows: a summary of the current state of knowledge of the physical and dynamical properties of Apophis is presented in §3, as is a description of the geometry pre- and post the April encounter. Section 4 summarizes the current literature about the effects of the Apophis-Earth encounter, effects on Apophis's orbital and spin state evolution, as well as more subtle surface changes and potential deformation. We then introduce in §5 and 6 the wide range of ground and space observations that would help monitor the effects presented in section 4. Conclusions and recommendations are provided in §7. Finally a hazard assessment of the effect of space contacts with Apophis is presented in §8.

3. BACKGROUND

In order to provide context and background for the subsequent sections, we first outline the geometry of the close encounter and summarize the current state of knowledge about Apophis.

3.1. *Close Approach in 2029*

On April 13, 2029 Apophis will have a close approach with Earth, coming within a geocentric distance of $\sim 38{,}000$ km. Immediately prior to the close encounter, Apophis will approach exterior to Earth's orbit (the night side) and will be below the ecliptic plane. After the close approach, Apophis will be interior to Earth's orbit and above the ecliptic plane (Figure 1). The asteroid gets closer than geosynchronous satellites, though it does not pass through the belt (Figure 2). Apophis also encounters the Moon at 0.25 lunar distances on April 14, ∼17 hours after the 0.1 lunar distances encounter with Earth.

Figure 3 shows currently known Near Earth Asteroids (NEAs) that will come within five lunar distances over the next ten years. Notably, there are six fairly large objects that come within 5 lunar distances. (153814) 2001 WN5 (diameter $\sim$ 930 m) is the largest and approaches within 0.65 lunar distances on June 26, 2028. Apophis's 2029 close approach is significantly closer than the other known close approaches.

3.2. *Current state of knowledge about Apophis*

Orbit: The story of the Apophis orbit has been unique even from its discovery in June of 2004 by R.A. Tucker, D.J. Tholen, and F. Bernardi at Kitt Peak in Arizona. The object was lost due to a short and problematic data arc, and rediscovered in December 2004 by the Siding Spring Survey in Australia. Apophis gained public interest after it was recognized that there was a $\sim$3% chance of impact on April 13, 2029. This situation lasted only a few days, at which point pre-discovery observations dating to March 2004 were reported by the Spacewatch Survey allowing the 2029 impact to be ruled out. At this point the focus turned to the possibility of impacts after 2029, when the prediction uncertainty skyrocketed (Chesley 2006). Radar ranging measurements from Arecibo with 600 m resolution were crucial in establishing the close approach distance in 2029 of 5.6$\pm$1.6 Earth radii from the geocenter (Giorgini et al. 2008).

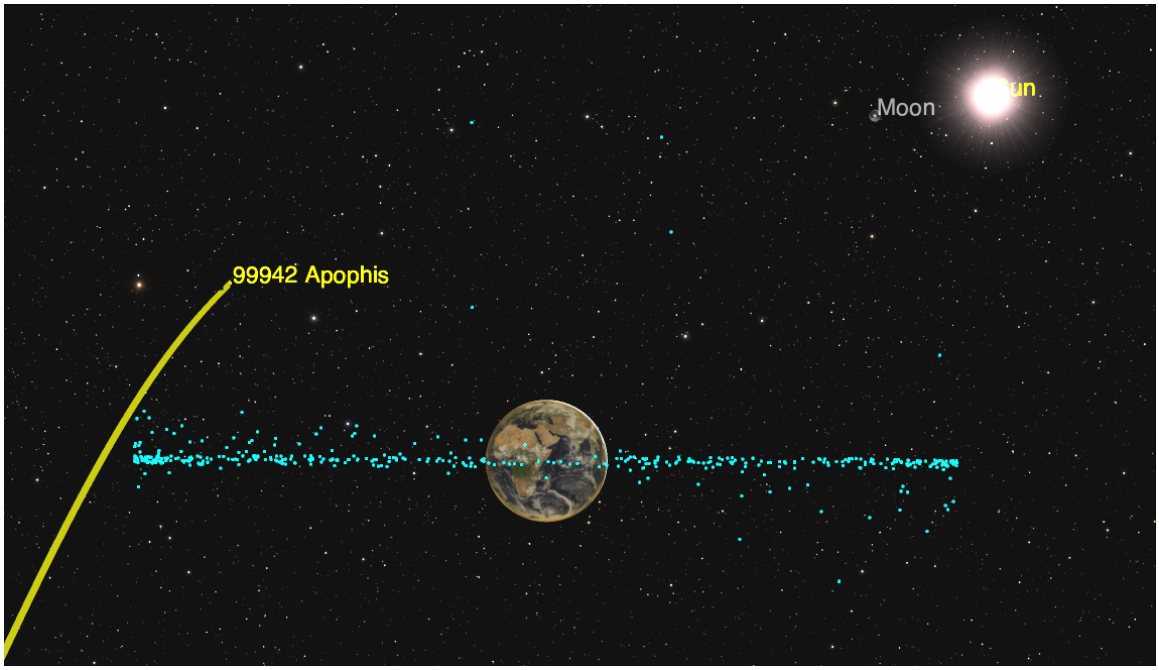

Figure 2. Relative geometry of the Apophis's approach with respect to the Earth, Moon, and Sun. Apophis is approaching from the night side and flying toward the Sun. Apophis is within the geosynchronous ring of satellites and above the plane at the time of the closest approach on 2029 Apr 13 at 21:46 UTC. Apophis will make the closest approach with respect to the Moon on 2029 April 14 at 14:32 UTC. Figure generated with Cosmographia software using SPICE (Acton et al. 2018).

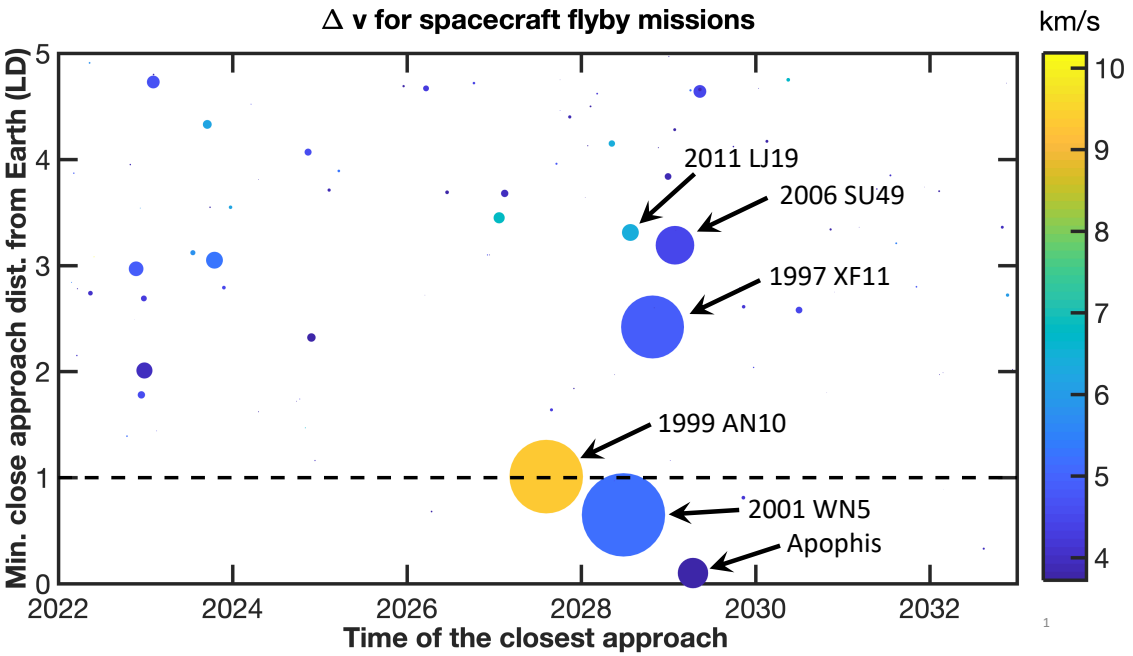

Figure 3. Closely approaching NEAs in the next ten years. The horizontal axis shows the year of the closest approach to Earth and the vertical axis shows minimum approach distance expressed in lunar distances (380,000 km). The circle sizes are scaled to correspond to the relative object sizes. The color corresponds to the Δv necessary for a flyby mission according to a simplified calculation in Shoemaker & Helin (1978).

The Yarkovsky effect remained a dominant source of orbital uncertainty until recently. Farnocchia et al. (2013) used probability distributions of various physical properties to model the Yarkovsky effect and found that the largest impact probability at that time was of order 10^{-6} for the year 2068. This estimate was refined upwards by a factor or a few by Vokrouhlický et al. (2015) based on detailed modeling of the non-principal axis spin state, but the Yarkovsky effect was still not clearly discernible from the astrometry. Later, leveraging precision radar and optical astrometry through 2020, Tholen & Farnocchia (2020) were able to unambiguously estimate the Yarkovsky acceleration, which was similar to predicted values; however, the 2068 potential impact persisted (Chesley & Farnocchia 2020). The incorporation of radar astrometry from 2021 into the orbital fit finally allowed the 2068 impact to be ruled out, and moreover ruled out all impacts for the next 100 years (Farnocchia & Chesley 2022). Thus Apophis was removed from JPL's Sentry Risk Page [1] for the first time since its discovery 17 years earlier. Also, at this point the Yarkovsky effect was unambiguously detectected with an SNR∼150 (Farnocchia & Chesley 2022).

Rotation State: An apparent slow rotation period of $P_1 \sim 30.6$ h was first reported by Behrend (2005) based on optical lightcurves. An extensive optical data set

[1] https://cneos.jpl.nasa.gov/sentry/

obtained by Pravec et al. (2014) refined the rotation period, and determined that Apophis is a tumbler in a moderately excited Short Axis Mode (SAM) state. As a non-principal axis (NPA) rotator, the orientation of Apophis does not repeat itself on the plane-of-sky. The precession period of the short axis around the angular momentum vector is $P_\phi = 27.38 \pm 0.07$ hours. The asteroid also has the second period due to a rocking motion, back and forth around the long axis, of P_ψ=263 ± 6 hours. These two periods relate to the originally measured period of 30.6 hours as $1/P_1 = 1/P_\phi + 1/P_\psi$. P_1 period is equivalent to the long axis precessing about the angular momentum vector, and it corresponds to the strongest signal in the lightcurves. Radar observations in 2012/2013 were able to confirm this spin state, although they were not sufficient to refine it. A refined spin state, which includes data from the 2021 optical apparition, was recently published by Lee et al. (2022). The new period values for the NPA short axis convention (see Samarasinha & Mueller (2015) for definitions) are P_ϕ=27.3855±0.0003 hours and P_ψ=264.18±0.03 hours. More data exist from 2020/2021 optical apparition (P. Pravec, pers. comm.), but the results have not yet been published.

The non-principal axis rotation represents a serendipitous window into the interior of Apophis. The Euler equations (Landau & Lifshitz 1976) used to model the spin state include moment of inertia ratios, I_{long}/I_{short} and I_{inter}/I_{short}. If the dynamical axes are different from the ratios derived from the uniform density shape model, a case can be made for a non-uniform density distribution inside the object. Pravec et al. (2014) and Brozović et al. (2018) both suggested that the differences for Apophis are smaller than 10%. The most recent lightcurve analysis (Lee et al. 2022) moderately improved these constraints. The values of the dynamical and shape ratios are: a_{dyn}/c_{dyn}=1.48±0.19, b_{dyn}/c_{dyn}=1.06±0.04 and a_{shape}/c_{shape}=1.56±0.04, b_{shape}/c_{shape}=1.12±0.03. These are self-consistent to ∼5%, and thus support homogeneous mass distribution.

Size: Radar is the only routinely-used ground-based technique that directly reveals the size of an object because it measures the line-of-sight time-delay (range) as the radar signal bounces from various parts of the object. Lightcurves cannot provide the size of an object, just the ratio of the principal axes. Infrared thermal observations require properly calibrated models, although the IR size estimates have excellent track record, and are accurate to ∼ 15% (Mainzer et al. 2011, 2015; Nugent et al. 2016; Masiero et al. 2018, 2020). Stellar occultations can also directly determine the object's size, but these are difficult to achieve for NEAs that are only several hundred meters in size (see Section 5.3.5).

To date, Apophis's size was determined by a variety of techniques. Delbò et al. (2007) reported a diameter of 270 ± 60 m based on the absolute magnitude and an albedo estimate. This was followed by the size estimate from the infrared

thermal studies by Müller et al. (2014) and Licandro et al. (2016), 375^{+14}_{-10} m and $380 - 393$ m respectively. Radar observations from 2012 and 2013 placed a lower bound on the long axis of 450 m, and yielded an equivalent diameter of 340 ± 40 m (Brozović et al. 2018). The latest size determination based on thermal modeling of NEOWISE data was published by Satpathy et al. (2022), 340 ± 70 m, in agreement with radar measurements.

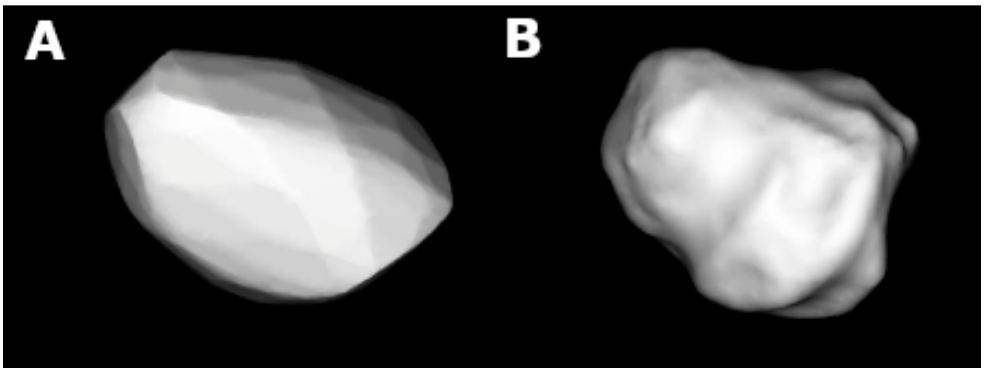

Figure 4. A) Convex shape of Apophis based on lightcurves (Pravec et al. 2014). B) Bioblate shape of Apophis based on radar data (Brozović et al. 2018).The principal difference is that lightcurves only provided a convex shape of the object.

Shape: The rotational lightcurves obtained in 2005 by Behrend et al. revealed an amplitude of 0.95 mag, suggesting that Apophis is an elongated object. Apophis was extensively observed in 2012 and 2013 by both lightcurves photometry and radar. The first shape model of Apophis was published by Pravec et al. (2014) (Figure 4), with principal axes ratios $a/c = 1.64 \pm 0.09$ and $b/c = 1.14^{+0.04}_{-0.08}$, where a, b, and c and the long, intermediate, and short axes. Goldstone delay-Doppler images of Apophis with 18.75 m effective resolution revealed that the echo was bifurcated in certain plane-of-sky orientations, suggesting a bilobed shape (Figure 5). The inversion of radar data produced the peanut-shape model in Figure 4.

In general, radar data suggest that at least 15% of NEAs larger than 200 m in diameter are bilobed in shape and have bimodal mass distribution (Brozović et al. 2010). Radar imaging allowed the identification of more than 70 NEAs of this type to date. Contact binaries tend to have relatively slow rotation periods (>10 hours), and some of them are known to have excited spin states (Hudson & Ostro 1995; Rivera-Valentín et al. 2019). Thus, if Apophis is a contact binary, it belongs to a relatively common type of NEA shapes.

Composition: Binzel et al. (2009) conducted one of the very first detailed mineralogical studies by analysing Apophis's visible and near-infrared (0.55 to 2.45 μm) reflectance spectrum. They found Apophis to be an Sq-class asteroid, with a spectrum closely resembling LL ordinary chondrite meteorites. They suggested

Apophis has an olivine to pyroxene abundance ratio (ol/(ol+px)) ranging from 0.65 to 0.75. They further compared Apophis to (25143) Itokawa and identified composition and size similarities. Reddy et al. (2018) found similar results and determined the probability of Apophis to having similar composition to a LL chondrite was 99% based on the inferred olivine (Fa number) and pyroxene (Fs number) mineralogy.

Mass: The mass of Apophis has not been estimated to date, although the current high precision measurement of the Yarkovsky acceleration can put some constraints. The leading source of the uncertainty is thermal inertia, that is currently constrained to 0-340 in SI units (3σ) Yu et al. (2017). Previously published papers (Müller et al. 2014; Licandro et al. 2016) had different values, 250-800 SI and 50-500 SI units respectively. The bottom line is that it is very difficult to constrain thermal inertia from the current observations (mid-infrared observations from CanariCam on Gran Telescopio CANARIAS and far-infrared data from PACS on Herschel). Apophis's slow rotation period of 30.6 hours contributes to the difficulty of these IR observations.

Radar scattering properties can provide some estimate of the near surface bulk density. The bulk density is a combination of near-surface porosity and solid density. If we combine the Goldstone radar albedo for Apophis of 0.25 ± 0.11 with Eros-calibrated expression for the near-surface solid density from equation 15 in Magri et al. (2001), we obtain 3.75 g/cm^3 for the assumed porosity of zero. The uncertainty on this value is at least several tens of percent due to the assumptions in the density formula and due to the uncertainties in radar albedo. However, radar-estimated solid density is not far from the density estimate for LL chondrite of 3.5 g/cm^3 (Britt et al. 2002). If we combine the LL chondrite density with a ∼340 m diameter, we obtain an upper bound on mass of $\sim 7 \times 10^{10}$ kg. The mass of Apophis is almost certainly lower than this, given that most asteroids are rubble piles. For example, Margot et al. (2015) reported a significant internal macroporosity, on the order of 50%, at least for the case of NEA binaries.

4. EFFECTS OF THE 2029 EARTH ENCOUNTER ON APOPHIS

Predictions about the effects on Apophis as a result of the Earth encounter and the magnitude of any resulting changes have been made using a variety of modeling approaches including treating Apophis as a rigid body (e.g. Scheeres et al. (2005)), as a self-gravitating granular aggregate (e.g. DeMartini et al. (2019)), and utilizing finite element modeling (e.g Hirabayashi et al. (2021)). The outcomes of these approaches vary in their details, but there are overall trends which inform the observational opportunity afforded by the close approach. The overall trends in the predictions,

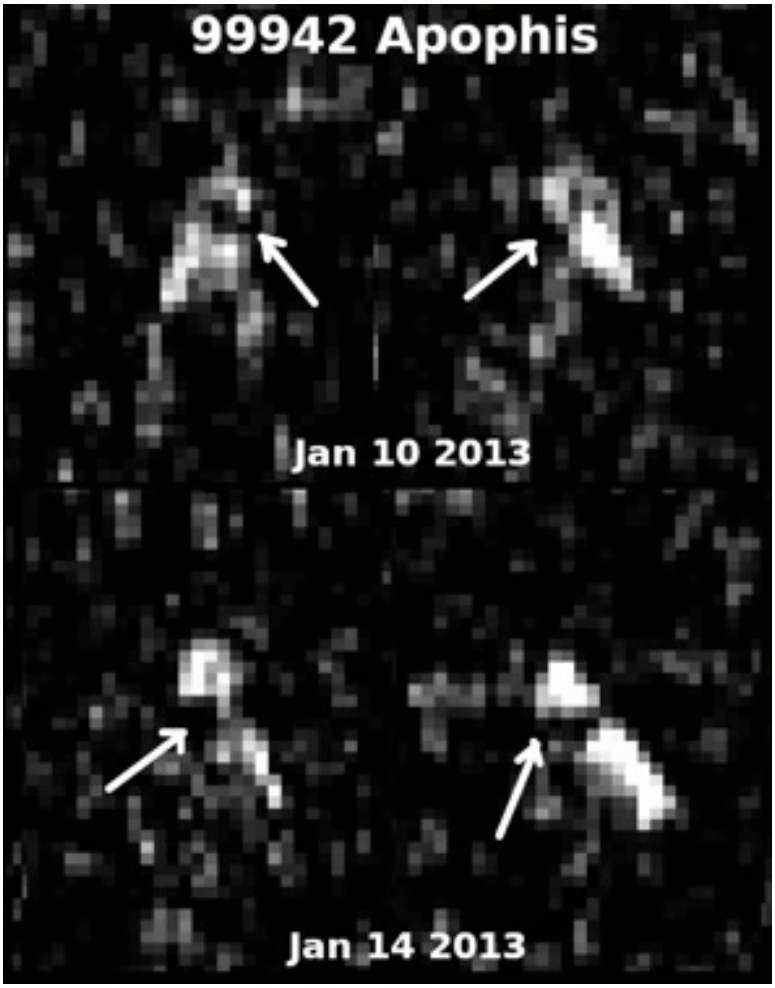

Figure 5. Goldstone delay-Doppler images of 99942 Apophis from the 2012–2013 apparition (modified from Brozović et al. (2018)). Time delay (range) increases from top to bottom and Doppler frequency increases from left to right. The range pixel resolution is 18.75 m. Each panel contains about 100 minutes of data integration. The arrow points to a bifurcation in the radar echo.

from the most likely (and larger magnitude effect) to the least likely (and smaller magnitude effect) are:

- Apophis's orbit will change from an Aten orbit to an Apollo orbit.
- Apophis's spin state will most likely change significantly.
- Apophis may experience localized areas of resurfacing.
- Apophis might experience small changes in shape.

The quantitative details of the predicted effects vary from model to model and are, in general, sensitive to uncertainties about Apophis's shape, internal structure, and rotational state during the close approach. One of the largest uncertainties cited by many models is the orientation of the asteroid during close approach. All the currently

available published predictions used the rotation state of Pravec et al. (2014). No predictions are currently available which use the updated spin state of Lee et al. (2022). The updated spin state has smaller uncertainties, so it is expected to yield tighter constraints on Apophis's orientation in 2029. However, more detailed analyses of the uncertainties in 2029 are needed to quantify the impact of this improved state of knowledge on predictions of the outcome of the encounter.

Furthermore, the radar shape of Apophis would be consistent with, but does not require, a significantly bifurcated shape or even a contact binary. Several authors have speculated on how the effects of the 2029 Earth encounter would vary if Apophis were a contact binary (e.g. Scheeres et al. (2020); Hirabayashi et al. (2021)); however no detailed modeling efforts to date have evaluated such configuration. In general, the studies which have mentioned this possibility propose that a contact binary asteroid would experience larger effects from an Earth encounter than other internal configurations, particularly resulting in larger areas of resurfacing and larger possible changes in shape.

The subsections that follow discuss several of the representative models and their predictions.

4.1. *Orbit*

As discussed above, the 2029 encounter of Apophis is highly unusual for the combination of asteroid size and proximity to Earth. Indeed, the orbital perturbation from Earth's gravity on the Apophis orbit is enough to change the orbital class of Apophis from Aten to Apollo, given the fact that the semimajor axis of the orbit will jump from 0.92 au to 1.10 au at the time of the 2029 encounter. The perihelion distance will also increase, from 0.74 au to 0.89 au, and other orbital parameters will change to varying extents. (see Figure 6) In addition to the change in the orbit of Apophis, a crucial aspect of the 2029 encounter is the dramatic increase in orbital uncertainty when mapping through the 2029 encounter to make predictions at subsequent encounters. While we can say with confidence that the change in the orbit due to the 2029 encounter will be large, we do lose a significant amount of orbital precision when passing through the encounter. For example, the uncertainty in orbital period grows by a factor over 3000× during the encounter, which causes the prediction uncertainty to spread far more rapidly along the orbit compared with the pre-encounter growth in position uncertainty. This property, of course, is what allowed Apophis to remain as a potential impactor for so many years after discovery.

4.2. *Spin State*

The effect of the close encounter on Apophis's spin state has been modeled, starting with Scheeres et al. (2005) by several teams since the asteroid's discovery - with increasingly sophisticated models and significant improvements about the body's physical characteristics. While the details of the models and the state of knowledge about Apophis have changed, the overwhelming conclusion is that Apophis's spin state

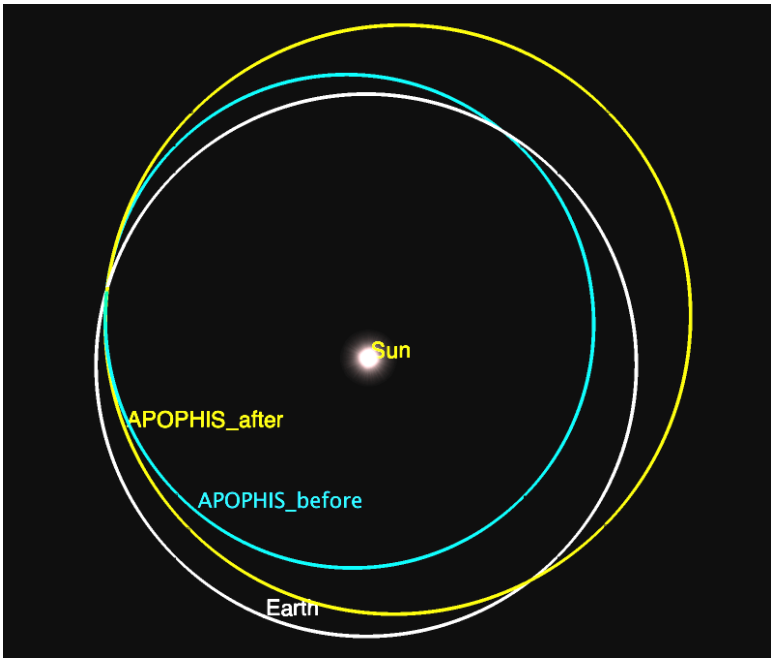

Figure 6. Apophis heliocentric orbit change (top-view) due to the 2029 encounter with Earth. Figure generated with Cosmographia software using SPICE (Acton et al. 2018).

could undergo a major change - but the details of exactly how it will change depend critically on the orientation of Apophis during the close encounter. While the spin state has been measured (Pravec et al. 2014), the uncertainties are too large to adequately constrain the encounter geometry - resulting in a wide range of estimates of the magnitude of the change in spin state. The more recent spin state reported by Lee et al. (2022), which reports reduced uncertainty in Apophis's spin state, has not yet been incorporated into models which predict the change in spin state during the close encounter. This refined spin state may still not be precise enough to constrain the orientation uncertainties in 2029.

Scheeres et al. (2005) performed an early assessment of the 2029 encounter's effect on the asteroid's spin. Using the physical parameters available at the time, and treating Apophis as a rigid body, the authors concluded that the asteroid will experience significant angular accelerations during the encounter and that the spin state is likely to change. They also showed a clear correlation between the conditions during the close approach (geometry, moments of inertia, and the initial rotation state of Apophis) and the final spin state.

In a recent study, DeMartini et al. (2019) used a discrete element model of self-gravitating granular aggregates of identical spheres in a hexagonal close packed configuration subject only to gravitational and soft-sphere contact forces. Using the 2018 radar shape model of Brozović et al. (2018), they found that the change in period depended strongly on the orientation during encounter - ranging from a minimum change of -7.603 hours to a maximum change of 14.440 hours. In addition, DeMartini

et al. (2019) considered a range of plausible asteroid densities and found little to no effect on the change in rotation period. In subsequent work, DeMartini et al. (2021) repeated the analysis using a random polydisperse packing instead of hexagonal close packing, effectively changing the angle of internal friction and shear strength of the aggregate. This revised model predicts a substantial spin change of +/- 20% of the current average spin period.

Spin state changes due to Earth encounters have previously been observed in Toutatis (Takahashi et al. 2013) and Duende (Benson et al. 2020). The spin state of Toutatis was measured both before and after the change. Modeling the change enabled Takahashi et al. (2013) to significantly reduce the uncertainty in the ratios of moments of inertia. (See §5.2 for more details.) In contrast, the spin state of Duende prior to the encounter was poorly constrained and well characterized after the encounter. Benson et al. (2020) utilized a model of the encounter to identify possible pre-encounter spin states. In both cases, modeling the change in spin state enabled a significant improvement in the state of knowledge about the asteroid.

Under a wide variety of assumptions, a substantial change in spin rate is predicted as a result of the close encounter. The data required to quantify this change in spin rate should be obtainable from ground based photometry and radar. Subsequent modeling of the measured effect would enable an enhanced assessment of the uniformity of Apophis's mass distribution. This analysis will also reveal any changes in the moment of inertia ratios pre-and post-encounter.

4.3. *Surface Change and Deformation*

The possibilities of surface change and/or deformation of Apophis due to tidal stresses have been studied utilizing a variety of approaches and assumptions about the asteroid.

As far as we understand at the moment, the shape of asteroid Apophis will not change unless its structure is extremely weak. The asteroid will remain outside the fluid Roche limit unless its density is below 440 kg/m^3 (Scheeres et al. 2005). If, on the other hand, Apophis is studied not as a fluid, but as a self-gravitating aggregate, able to sustain shear stress, the asteroid will only change its shape if its density is $<$250 kg/m^3, if its body is extremely elongated or if it has an angle of friction $< 5^\circ$ (Holsapple & Michel 2006). All these conditions are highly unlikely for a real asteroid.

As for its surface, most studies have modelled Apophis as an ellipsoid and have studied its surface through different numerical codes and theoretical approximations. They found that there is a possibility of small avalanches that could appear on its surface. The stability of the surface depends on the local slope, strength and particular packing of the particles and as a result, predicting exactly where avalanches are going to happen is not possible.

Yu et al. (2014) showed that the maximum change in slope angle is less than 2°. Which they also noted was not large enough to trigger any massive avalanches

throughout their simulated sand piles when subjected to the forces the asteroid would be subjected to during the flyby. Even in more extreme cases at approach distances as close as 2 Earth radii, their simulated Apophis did not experience any irreversible distortion. This happened because the duration of strong tidal effects is relatively short.

Further work done by Valvano et al. (2022) coincides with Yu et al. (2014), but also finds that the maximum change in slope could be up to 4° if the density of Apophis is lowered to 1290 kg/m^3. This means that whether or not there are avalanches on the surface will depend on the specific shape of the asteroid and the actual angle of repose of the surface, which is in turn directly related to its cohesive strength. Even in the best case scenario, surface flow is not expected to be major.

However, the latest shape model, based on ground radar observations, points to the existence of a neck which implies a bilobate body (Brozović et al. 2018). If this shape model is taken into consideration, the studies find that: 1. Rotational variations can change stress variations in Apophis. 2. Stress variations may be up to 0.5 Pa at maximum during the 2029 closest encounter. 3. The neck region, especially the concavity, is sensitive to stress variations (Hirabayashi et al. 2021).

DeMartini et al. (2021) utilized a discrete element model of self gravitating granular aggregates of identical spheres in a random polydisperse packing configuration consistent with the (Brozović et al. 2018) shape model. Their particles were subject to gravitational and soft-sphere contact forces. The predicted surface motion varied from motions on the scale of millimeters to motions of meter-scale surface boulders over distances similar to their radii, depending on the assumed regolith porosity, bulk Young's modulus, and orientation of the asteroid during the encounter.

A topic that has not yet been mentioned this far is the effect of Earth's magnetic field on electrostatically charged grains on the surface of Apophis. Electrostatic dust lofting was first hypothesized as a mechanism to produce the lunar horizon glow observed by the Surveyor spacecraft (Rennilson & Criswell 1974), Apollo light scattering observations (Glenar et al. 2011), and measurements by the Apollo 17 Lunar Ejecta and Micrometeorite experiment (Berg et al. 1973). Recent observations by the Change'E-3 mission also seem to support the hypothesis of electrostatic lofting (Yan et al. 2019).

There is no evidence of the presence of such grains existing (or levitating) on/over the surface of Apophis; however, if they do exist, 1. for grains that are currently levitating (or somehow moving above the surface), they will be subject to a force in the $\vec{v} \times \vec{B}$ direction, where $\vec{v}$ is the velocity of the particle and $\vec{B}$ is magnetic field. This could cause particles to accumulate in a different area than they had previously, but unless there are a lot of levitating particles, it probably wouldn't be a big effect.

2. When bodies pass through Earth's magnetotail, they get bombarded with higher energy electrons (as observed on the Moon)[2].

As an example of this effect, Hartzell et al. (2022) studied the possibility of electrostatic levitation as the cause of the ejected particle observed at Bennu. Electrostatic charging is still not well understood; however, there are at least two theoretical models that have had a degree of success. Wang et al. (2016) hypothesized that large electrostatic forces could be generated when electrons emitted from one particle accumulated on the surface of nearby particles. In this model, particles are taken as individual entities that can be illuminated on one side and produce shadows on other particles (the patched model). This is fundamentally different from considering them as small pieces on an infinite flat plane. Zimmerman et al. (2016), on the other hand, developed a theoretical model for the charging of particles given the above mentioned method. The fundamental property of this patched charge model is that it assumes electrons emitted from one particle will deposit onto a neighboring particle, producing large small-scale electric fields.

For an electrostatically charged particle to levitate, the electrostatic repulsive force has to overcome the particle's weight and cohesion. Given the random position of the grains on the surface of an asteroid (not to mention their varied shapes and sizes), one extreme scenario would be to have the weight and cohesive force exactly opposite to the electrostatic force. The weight is also affected by the rotation of the asteroid and the cohesive force depends on the specific chemistry of the grains and geometry of the grains (Persson & Biele 2022). The former can be calculated, but the latter requires some assumptions as detailed analysis of pristine asteroid samples do not exist, except for asteroids Itokawa and Ryugu.

Hartzell et al. (2022) concluded that submillimeter particles could be electrostatically levitated, but that the particles observed to be ejected from asteroid Bennu could not. If electrostatically charged particles exist on, or levitating on asteroid Apophis, models and assumptions could be confronted with an unprecedented experimental opportunity. This, however, would require observations by a nearby spacecraft with specialized instrumentation to detect such phenomena.

5. REMOTE OBSERVING OPPORTUNITIES

The opportunities for remote observing range from optical to radar wavelengths and utilize a variety of methods including imaging, spectroscopy, and polarimetry. While the SAT does not endorse or promote the use of particular facilities or instruments, we do discuss specific facilities and instruments in this section in order to illustrate the capabilities that are relevant.

5.1. *Close Approach Geometry*

[2] C. Hartzell's private communication

Apophis will approach Earth from southern declinations, move rapidly past Earth, and complete its outbound trajectory at a declination of +17°. Prior to the close approach, Apophis will be visible in the night sky from the southern hemisphere. Immediately prior to perigee, Apophis will be very bright (V $\sim$ 3) and visible by the unaided eye from south-west Europe and north-west Africa (See Figures 7, 11, and 12). The asteroid becomes a day-time object after the closest approach, and it remains within 45° from the Sun until late May. After perigee, ground based night time observing will be challenging due to the small solar elongation. Apophis is at opposition in the first week of December, as $\sim$ 17.5 magnitude object. This is the most likely time for extensive post-flyby optical observations from ground. Figure 8 shows radar observing windows from Goldstone (northern hemisphere) and Canberra (southern hemisphere) for the duration of the 2029 apparition. Radar observations are possible regardless of the solar elongation, but they are limited by the line-of-sight distance, because the SNRs are inversely proportional to the fourth power of distance. For example, when an object doubles its distance from radar, the SNRs get reduced by a factor of 16.

5.2. *Radar Observations*

The proximity of Apophis encounter in 2029 will make the asteroid an exceptionally strong radar target. The SNRs will exceed $> 10^6$ per day at multiple radar facilities (Figure 9). Radar observations could range from many routinely used (*i.e.* high-resolution delay-Doppler imaging, speckle observations, radar polarimetry) to novel observational techniques (*i.e.* deep sounding with long radar wavelengths) (Table 1). Some of the outstanding questions are Apophis's size and shape, and these could be determined to < 5 m precision by an extensive radar observing campaign.

Apophis's SNRs are suitable for ranging at facilities such as Goldstone's DSS-14 antenna from mid-March to mid-May. The high-resolution imaging will be possible for two weeks centered on the closest approach. The SNRs are sufficient to resolve the surface of Apophis with tens of thousands of pixels. This could reveal a variety of surface features such as ridges, concavities, grooves, and meters-sized boulders (see Fig. 9). The southern hemisphere radar facilities such as Canberra's 70-m antenna DSS-43 could also be observing Apophis as the asteroid is incoming from -30 deg in declination.

The proximity of Apophis's approach will allow observations from less-sensitive radar facilities that usually observe artificial satellites and orbital debris in lower-Earth and/or geosynchronous orbits, or study Earth's atmosphere. Many radar facilities are designed to track fast moving spacecraft (up to 0.25 deg/s on the plane of sky), so they would be capable to track Apophis that has a maximum angular rate of 0.01 deg/s during the closest approach. The ultra-short wavelength radars such as Haystack HUSIR radar could resolve the surface of Apophis down to a few-centimeter level, while the long-wavelength radars (Haynes et al. 2022) could penetrate the aster-

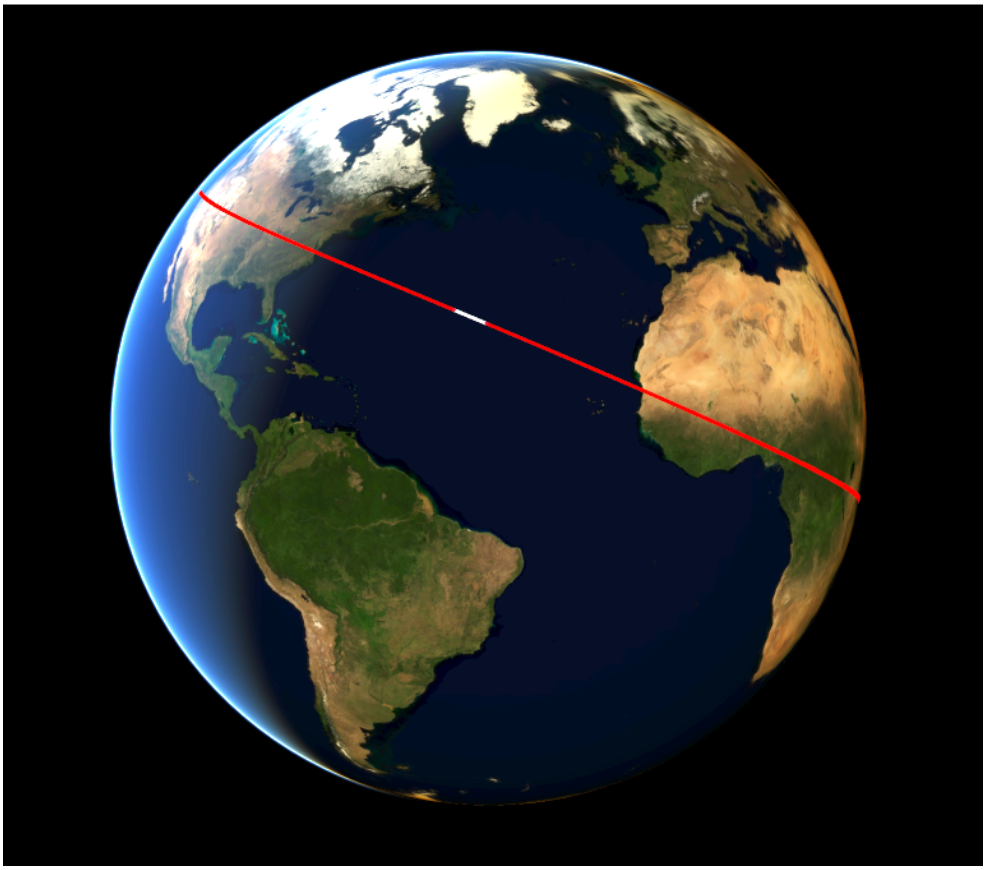

Figure 7. The ground track of Apophis during the close approach in 2029. The white swath marks the ground region where Apophis will be directly above during the minutes around the closest approach, 21:43 - 21:49 UTC. This is night-time for the west coasts of Europe and Africa, and day-time for the east coasts of the Americas. Apophis becomes a day-time object after the closest approach. Figure generated with Cosmographia software using SPICE (Acton et al. 2018).

oid's surface tens of meters in depth, and reveal its interior (Table 1). By 2029, some new radar capabilities will exist around the world (e.g. EISCAT 3D in the northern Scandinavia). It is also possible that there will be a radar capability at the Green Bank Telescope.

It is important to note that some radars use C-band (7190 MHz) transmitters, same as the frequency used for spacecraft communication. The ground based radar observations are unlikely to cause any interference with a possible spacecraft in the vicinity of Apophis, but there would have to be some plan (and advance testing) in place. The radar power density is of no concern for spacecraft because it drops to negligible levels after a few hundred kilometers (Jamnejad 2014). The X-band (8560 MHz) and S-band (2380 MHz) radar transmitters were used to illuminate spacecraft before, and there were no issues reported by the mission teams (NASA 1998; Brozović et al. 2017).

Tidal resurfacing of Apophis would be one of the most interesting outcomes of the 2029 close encounter. This is also very challenging to detect with ground-based

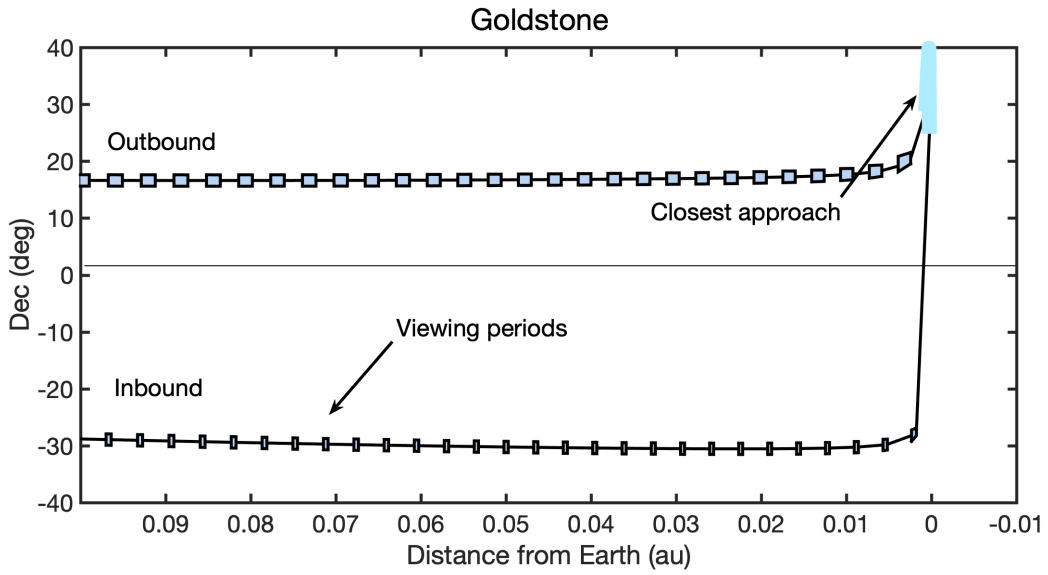

(a)

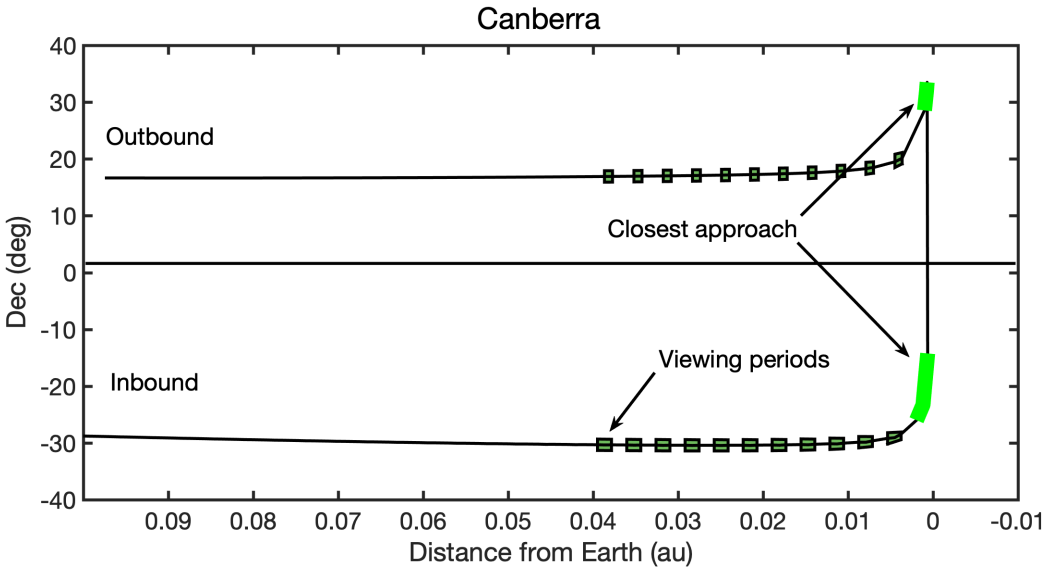

(b)

Figure 8. a) Observing windows (marked in blue) at Goldstone as Apophis is inbound/outbound ± 0.1 au. The vertical axis shows declination of the asteroid. Apophis will approach from the southern declination, rapidly move to the northern hemisphere during the closest approach, and keep northern declination of ∼ 17 deg after the closest approach. The expanded blue region along the vertical axis is Goldstone coverage at the time of the closest approach. Goldstone will be able to observe Apophis on April 13/14 21:46 - 01:57 UTC. Goldstone viewing periods are longer after the closest approach. From April 10–19, Apophis will be visible from Goldstone for more than 70 hours. b) Observing windows (marked in green) at Canberra. At Canberra, Apophis will only be detectable within ± 0.04 au due to less powerful transmitter at DSS-43. Canberra however, has an excellent coverage shortly before and after the closest approach. Canberra will be able to observe Apophis on April 13 08:50-17:58 UTC and on April 14 01:58-04:10 UTC (bright green vertical region).

techniques. High-resolution (meter and sub-meter) radar imaging may be able to

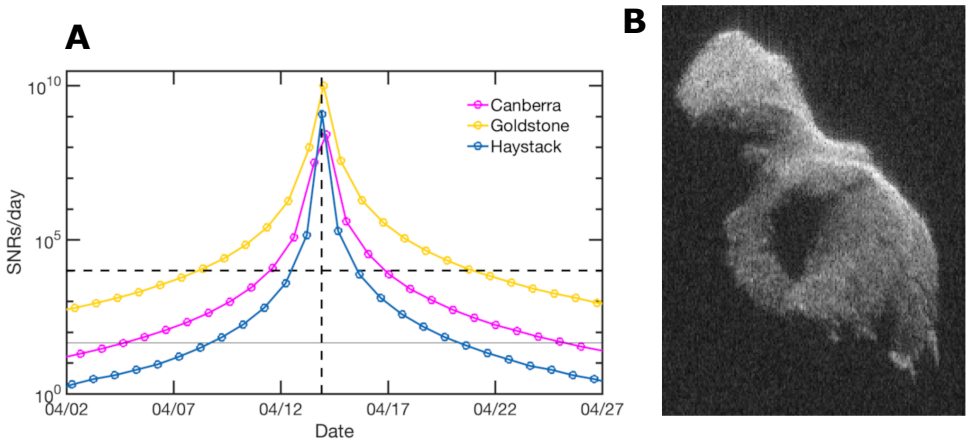

Figure 9. A) The signal-to-noise ratios (SNRs) estimates for Apophis in 2029 for Goldstone (DSS-14), Canberra (DSS-43), and Haystack (X-band HUSIR system). The SNRs are expressed in the units of standard deviation above the noise level. The light grey line marks the 2012/2013 SNRs, while the dashed line marks the SNRs needed for high-resolution (few meters and better) imaging.
B) An example delay-Doppler image with 3.75 m range resolution of a very strong radar target 2014 HQ124. Goldstone, DSS-14, was transmitting and Arecibo was receiving. This NEA is a similar size as Apophis with slow, ∼20 h rotation period. 2014 HQ124 is also a contact binary, perhaps similar to Apophis in shape. The SNRs for observations on 2014 June 08 exceeded 100,000 per day, and this image contains only 960 seconds of data. The asteroid was ∼3.7 lunar distance away at this time. The image reveals large concavity, decimeter-sized boulders, and even radar-dark surface feature that resembles a fissure on the surface (lower-right). (https://www.jpl.nasa.gov/images/pia18412-radar-images-of-asteroid-2014-hq124). The SNRs for Apophis in 2029 are strong enough to least double the number of pixels in range. Assuming systems like Haystack HUSIR radar, the surface could be resolved down to a few centimeters level.

detect such changes. Radar polarimetry could also be utilized. The transmitted radar signal is circularly polarized, and reflection from an object results in the echo polarized in the same sense (SC), or the opposite sense (OC) as the transmitted signal. Carter (2005) and Hickson et al. (2021) described how a sophisticated polarimetric analysis of high-SNRs delay-Doppler images via m-chi decomposition of the Stokes vector can reveal the scale and the shape of surface particles, and provide evidence for regolith deposits. The comparison of the polarimetric parameters pre- and post-flyby could reveal changes in surface properties due to tidal resurfacing.

The precision measurements of Apophis spin state pre- and post- flyby are of high interest because of the constraints that the NPA rotation gives with respect to the interior mass distribution. The comparison of the moment of inertia ratios pre- and post- flyby could also reveal if there were any changes in the interior. Lightcurves and radar imaging are commonly used methods for spin state determination. Radar speckle is another technique (Busch 2010). This approach yields instantaneous Euler angles (ϕ,θ,ψ) in time, and it leads to a more straightforward spin state estimate that does not require the full reconstruction of 3D shape model from radar imaging.

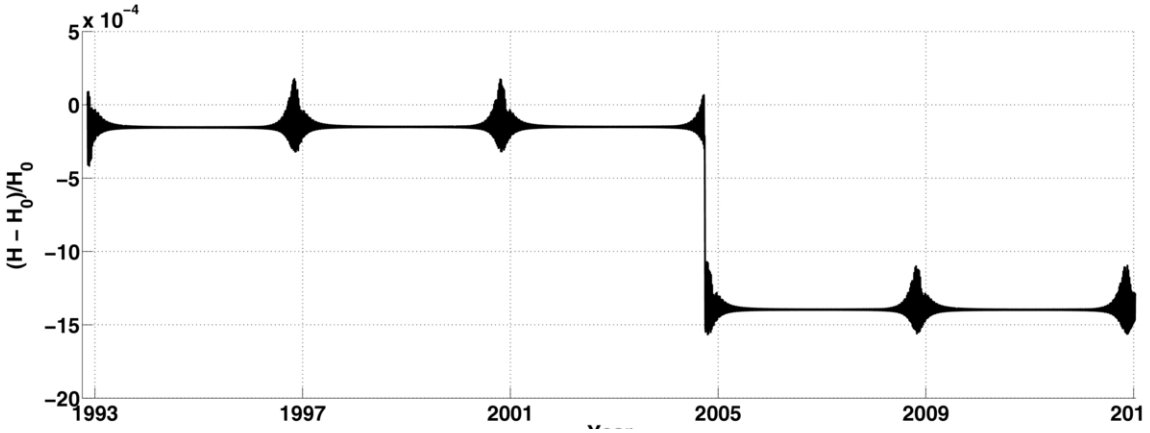

Figure 10. Change in the rotational angular momentum for NEA 4179 Toutatis due to periodic Earth flybys (Takahashi et al. 2013). The asteroid was observed by radar in 1992, 1996, 2000, 2004, and 2008. This yielded orientations of the asteroid at each apparition that allowed for dynamical modeling of the spin state evolution. The 2004 encounter at 3.9 lunar distance resulted in the most significant spin change. The spin alteration due to the Apophis's encounter with Earth will be orders of magnitude more dramatic.

Radar data were used in the past to determine the spin states of NPA rotators 4179 Toutatis and 214869 2007 PA8 (Hudson & Ostro 1995; Hudson et al. 2003; Brozović et al. 2017). The level of precision was high enough to conclude that both NEAs were spinning like uniform density objects to within several percent.

Takahashi et al. (2013) analysis of the spin state change of Toutatis due to tidal interaction with Earth during 3.9 lunar distances encounter in 2004 demonstrated that modeling of the spin evolution led to improved uncertainties on all spin parameters, including the ratios of moment of inertia (Figure 10). For example, the a priori uncertainty on I_{int}/I_{long} = improved by a factor of 3, from 3% to 1%. It is reasonable to assume that the spin state analysis for Apophis in 2029 would achieve at least this level of accuracy. Given the fact that Apophis radar data set could cover two months of observations, and that several meters level radar imaging could last for two weeks, it is likely that the precision would exceed 1%.

5.3. *Ground Based Optical and Near-IR Observations*

The 2029 flyby will present opportunities and challenges for ground-based observers (Figure 11). With a peak brightness of V∼3, Apophis will be accessible for study by almost any optical telescope on Earth. However, the high non-sidereal rates and the geometry of the flyby (e.g. solar elongation, declination) will require careful planning of pre and post encounter characterization. For example, hours after perigee Apophis will move into the daytime sky, thus complicating any investigation into the post-flyby state. Fortunately, Apophis becomes observable again in late 2029, reaching a

Table 1. Apophis science in 2029 enabled by ground-based radar facilities

Radar frequency	Immediate data products	Apophis science	Example Facilities	Current facility usage
>10 GHz	• cm-to-decimeter range resolution SURFACE imaging; • radar astrometry; • radar scattering properties and polarimetry	• super-small scale surface geology; • 3D-shape model reconstruction; • spin state; • moment of inertia ratios; • heliocentric orbit improvement; • cm-scale surface changes; near-surface roughness and bulk density; • radar albedo; • regolith deposits	HUSIR (Lincoln Labs)	Observations of space debris, LEO, and GEO targets; Observed one NEA to date (2012 DA14)
7–9 GHz	• 1.875 m and coarser range resolution SURFACE imaging; • radar astrometry; • radar scattering properties and polarimetry	• surface features and surface geology; • 3D-shape model reconstruction; • spin state; • moment of inertia ratios; • heliocentric orbit improvement; • meter-scale surface changes; • near-surface roughness and bulk density; • radar albedo; • regolith deposits.	Goldstone DSS-14 and DSS-13; Canberra DSS-43	Spacecraft communication; NEA observations are frequent and routine
10-500 MHz	• decimeter to tens of meters range resolution INTERIOR imaging; • radar scattering properties	• internal structure constraints: degree of homogeneity & porosity; • radar albedo	MISA, CMOR, OVRO, UNM–LWA, HAARP, ALTAIR, EISCAT 3D	Observations of Earth's atmosphere; • Observations of space debris, LEO, and GEO targets; • Proof-of concept stage for observations of NEAs

NOTE—HUSIR - Haystack Ultrawideband Satellite Imaging Radar, Massachusetts, USA;
DSN - Deep Space Network (antennas located at Goldstone, California, and Canberra, Australia are the most likely to be used for observations of Apophis);
Canberra DSS-43 currently only does Doppler-only observations, imaging capability needs to be established;
MISA - Millstone Hill Incoherent Scatter Radar, Massachusetts, USA;
CMOR - Canadian Meteor Orbit Radar, Ontario, CA;
OVRO - Owens Valley Radio Observatory, California, USA;
UNM - University of New Mexico Long Wavelength Array, New Mexico, USA;
HAARP - The High-frequency Active Auroral Research Program observatory, Alaska, USA;
ALTAIR - ARPA Long-Range Tracking and Instrumentation Radar, Kwajalein, Marshall Islands;
EISCAT 3D - European Incoherent Scatter Scientific Association, Finland, Norway and Sweden ;
LEO- lower-Earth orbit;
GEO- geosynchronous orbit

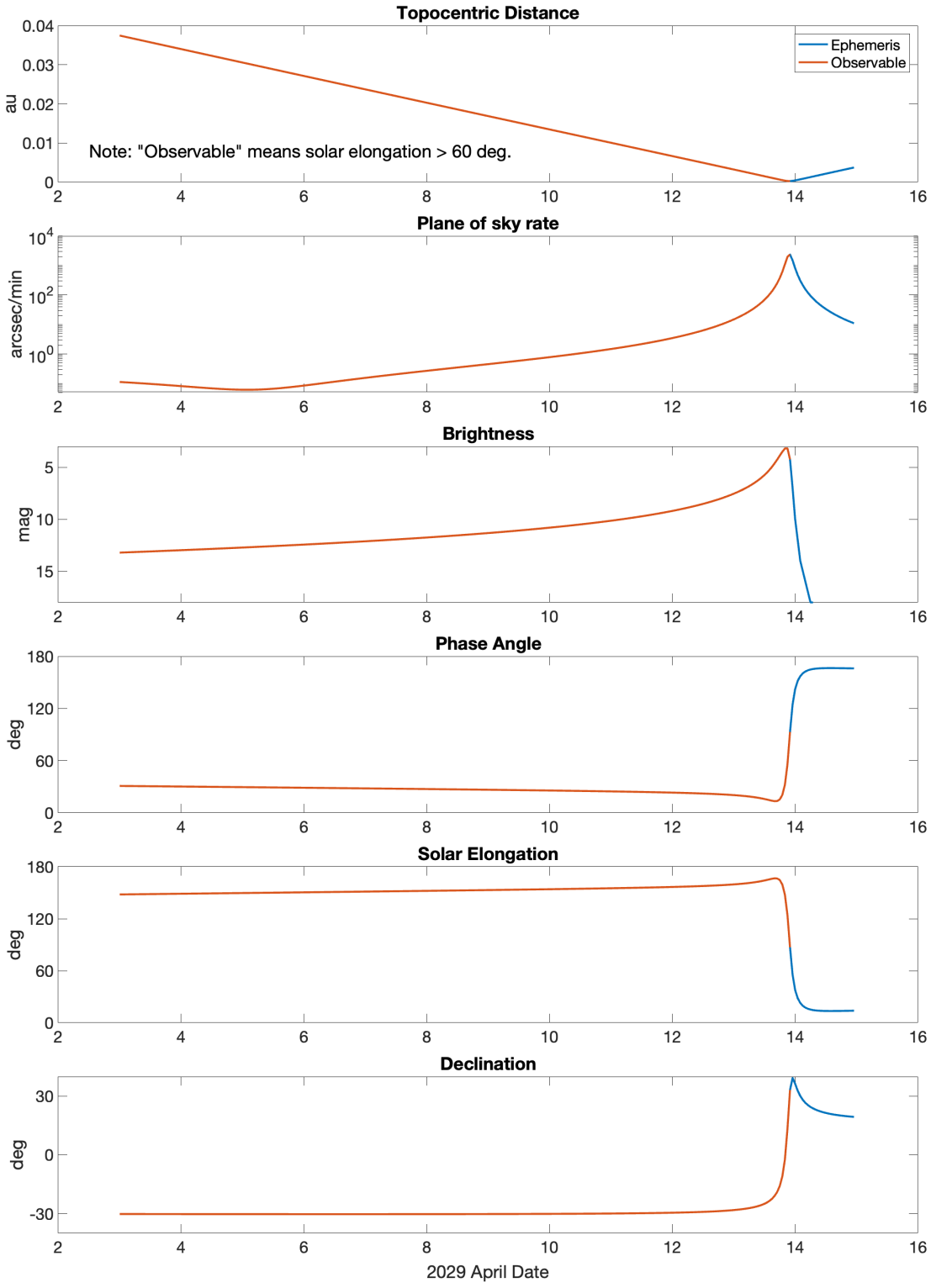

Figure 11. Observing geometry from the geocenter before and during the 2029 near-Earth encounter.

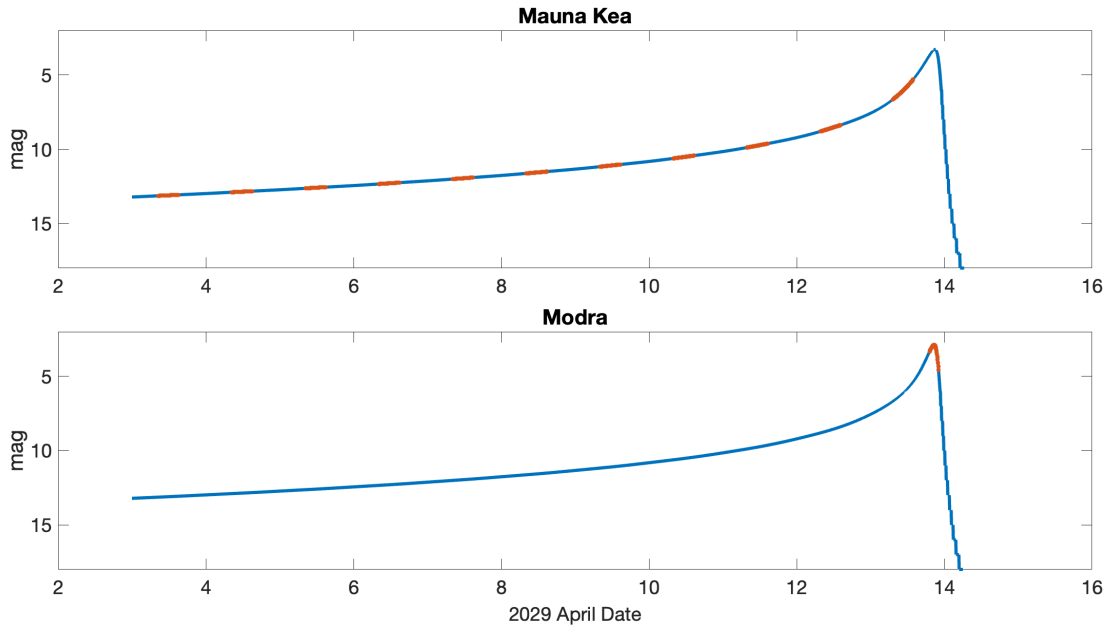

Figure 12. Observability of Apophis prior and immediately after the close approach from (top) Mauna Kea Observatories and (bottom) Modra, Slovakia. The red line delineates when it is nautical twilight or darker, the elevation is greater than 20°, and the solar elongation is greater than 60°.

peak brightness of $V \sim 17$ in November, thus providing additional opportunity for post-encounter studies.

Given the brightness of Apophis in 2029, there will be few limitations on techniques available for characterization, and there will not be a strong need to rely exclusively on large aperture facilities. For example, a simple CCD camera on a portable 8" Celestron strategically deployed in a favorable location, could collect lightcurve photometry that witnesses changes in spin state. We discuss here a range of techniques that can provide insight on such changes to the physical state of Apophis. Also noted are limitations and/or areas where advances in analysis procedures are required ahead of 2029 to realize the fully utility of a specific technique.

5.3.1. *Rotational Lightcurve Photometry*

The wide availability of telescopes and instruments capable of lightcurve photometry will inevitably lead to the collection of large volumes of imaging data on Apophis in 2029. It is important to note that optical lightcurves already provided an impressive level of accuracy for the pre-encounter spin state of Apophis (Pravec et al. 2014; Lee et al. 2022). The combination of extensive lightcurve coverage in the days and weeks surrounding flyby with high precision radar data represents an important synergy that will maximize scientific return.

A long baseline of lightcurve coverage will be required to unambiguously constrain the spin state of Apophis. The near-Earth flyby at $\sim$ 4 Earth radii of asteroid (367 943) Duende in 2013 is a useful analog to inform expectations for Apophis.

Like Apophis, Duende has a roughly 2:1 axis ratio and is in a slow (P_Φ = 8.71h, P_Ψ = 23.7h), short-axis mode (SAM), non-principal axis rotation state (Moskovitz et al. 2020; Benson et al. 2020). Constraining the post-flyby spin state of Duende was possible due to nearly three days of continuous lightcurve coverage, or about a factor of three times the longest rotational mode. Extending this analogy to the even longer periods associated with Apophis's spin state (Pravec et al. 2014) suggests that nearly a month of lightcurve photometry would be needed to constrain the spin state with lightcurves alone.

5.3.2. *Spectroscopy*

Apophis is classified as an Sq-type asteroid with compositional affinity to LL ordinary chondrites (Binzel et al. 2009; Reddy et al. 2018). This is similar to the asteroid 25143 Itokawa for which samples were returned to Earth by JAXA's Hayabusa mission (Nakamura et al. 2011). As such there is well founded understanding of the mineralogy and the effects of space weathering for such bodies. If the Earth encounter causes shifting of surface material on Apophis, then sub-surface material that is either unweathered or has different characteristics (e.g. grain size) could be freshly exposed. Exposing of fresh or texturally different material could manifest as changes in Apophis's reflectance spectrum. Ground based spectra of asteroids, when carefully controlled for instrumental systematics can achieve accuracy of a few percent in spectral slope (e.g. Devogèle et al. 2020) and $\sim$ 1% in absorption band parameters (e.g. Leith et al. 2017) at visible (0.5-0.8 microns) and near-infrared (0.8-2.5 microns) wavelengths. The latter translates to constraints on weathering state and composition that are accurate to a few percent (e.g. Reddy et al. 2018). Reddy et al. (2018) also proposed that Band I could serve as a baseline for identifying surface changes (i.e. freshly exposed surfaces) due to seismic shaking that may occur during the 2029 close encounter with Earth.

However, any changes to Apophis's surface are expected to be highly localized (e.g. Yu et al. (2014), see §4.3) and thus may be difficult to detect with unresolved observations from the ground. Modeling efforts to understand the physical extent of surface modification, *i.e.* fraction of the surface affected, and whether such changes could be spectroscopically detected in hemispherical averages of an unresolved source would be valuable leading up to 2029.

5.3.3. *Polarimetry*

The optical polarization ratio for asteroids, a quantity that expresses the relative contribution of parallel and perpendicularly polarized components of a measured signal, is correlated with surface properties such as albedo and grain size (Muinonen et al. 2002). The polarization ratio is often interpreted as a function of viewing geometry or solar phase angle (e.g. Cellino et al. 1999), though more recent work has shown the sub-hemispherical surface features can be resolved with polarimetric data. For example, Borisov et al. (2018) showed that the relative polarization, a quantity

that is independent of asteroid shape, varied periodically with rotation period for the near-Earth asteroid (4200) Phaethon. Maxima and minima in this polarization signature seem to align with radar-resolved features such as boulders, craters, and ridges (Taylor et al. 2019). This suggests strong promise for polarimetry as a technique to detect sub-hemispherical surface features and changes in surface features on unresolved sources.

However, despite its potential utility, there are two main hurdles to wider adoption of polarimetry for the purposes of characterizing asteroid surfaces. First, there are relatively few imaging polarimeters available to the observing community. Second, there does not yet exist a comprehensive theory to describe polarimetric light scattering by regolithic surfaces (for example, there does not currently exist an albedo-polarization relationship for asteroids viewed at high solar phase angles common to NEOs). Future investment in new polarimetric instrumentation and analysis tools will be needed to fully realize the potential of this technique for the 2029 Apophis flyby.

5.3.4. *High Resolution Imaging*

During its close encounter with Earth, Apophis will become a resolved source for instruments capable of high resolution optical imaging (Figure 13). At perigee Apophis will have an angular size larger than 1.8 arcseconds. This is well within the resolution limit of adaptive optics and speckle imaging instruments. As representative examples: the extreme adaptive optics instrument SPHERE (Beuzit et al. 2019) with the ZIMPOL camera (Schmid et al. 2018) at ESO's 8.2-m Very Large Telescope (VLT) is capable of imaging at close to the diffraction limit at visible wavelengths (< 0.02") , while the Quad-camera Wavefront-sensing Six-channel Speckle Interferometer (QWSSI; Clark et al. 2020) is capable of achieving a similar limit on the 4.3 m Lowell Discovery Telescope (LDT). (See Figure 14 for an example of high resolution imaging of an asteroid.) These instruments would resolve Apophis as a source many tens of resolution elements across, which translates to $\sim$ 10-m resolution on the surface. Optical and radar images complement each other, the first being an intuitive plane-of-sky image, and the second being a delay-Doppler image with resolution that surpasses that of an optical image by many fold (Figure 14). *Shape* software (Hudson 1994; Magri et al. 2007), used for the inversion of radar delay-Doppler images into 3D models, is also capable of ingesting the information from plane-of-sky images as well as from lightcurves.

Achieving closed loop corrections with adaptive optics (AO) systems may be challenging for Apophis. The high non-sidereal motion will make it impossible to use a field star(s) for AO correction. However, AO systems should be able to achieve closed-loop corrections with a laser guide star at the non-sidereal rates of Apophis (assuming the telescope can track the asteroid). For modern Alt-Az telescopes there is little practical difference in tracking at sidereal rates (15 arcsec/sec) versus maximum Apophis rates (> 20 arcsec/sec), so this could be a feasible technique for high resolution imaging throughout the encounter.

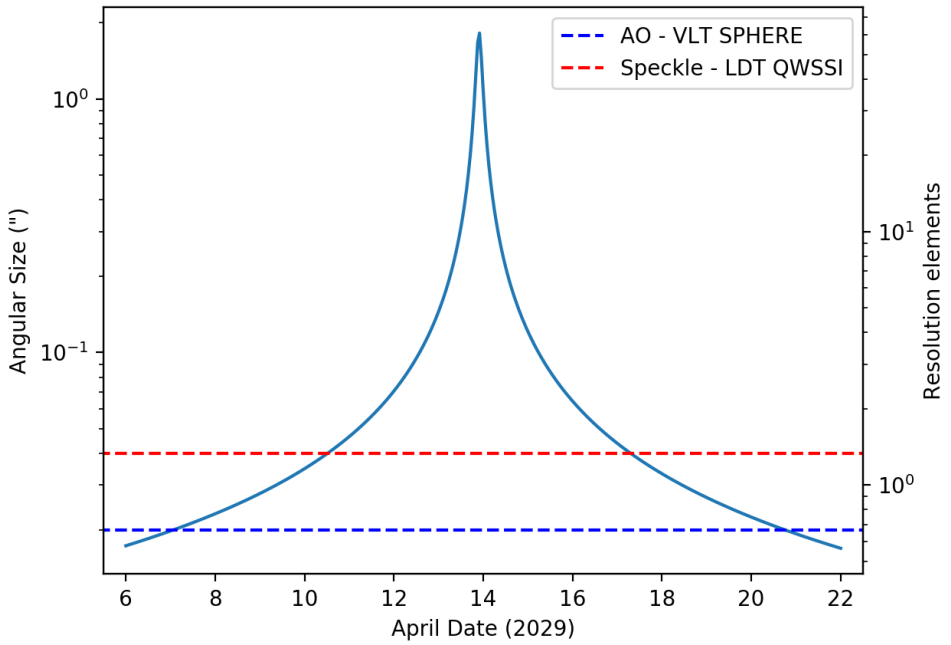

Figure 13. Angular size of Apophis as seen from the geocenter in the days surrounding its perigee passage in 2029. Representative resolution limits are shown for two different instruments: the extreme adaptive optics SPHERE instrument at ESO's 8.2 m VLT (Beuzit et al. 2019), and the QWSSI speckle camera at the 4.3 m LDT (Clark et al. 2020). The number of resolution elements (2nd y-axis) assumes an intermediate resolution limit of 30 mas.

Speckle imaging involves high cadence imaging to freeze phase fluctuations induced by the turbulent atmosphere on the incoming wavefront. Fourier analysis of these speckle patterns can yield high-resolution (approaching the diffraction limit) information about the source image. Recent realizations of speckle cameras have leveraged largely off-the-shelf hardware at relatively low cost (e.g. Clark et al. 2020). In addition, the relatively compact size of speckle cameras enables deployment at a wide range of telescope sizes. This flexibility could be leveraged for Apophis with a network of speckle cameras on portable telescopes, analogous to occultation networks (e.g. Buie & Keller 2016), that could be strategically placed to image rotational changes and surface modification in the few hours surrounding perigee. While the hardware to support speckle systems is fairly mainstream, a primary limitation to generating resolved images of objects with complex shapes, such as asteroids, is a need for further development in data processing algorithms. Shape reconstruction of an asteroid from a speckle data cube is a non-trivial process and is computationally expensive, though there have been recent advances in this area presented at conferences (Trilling et al. 2022).

5.3.5. *Stellar occultations*

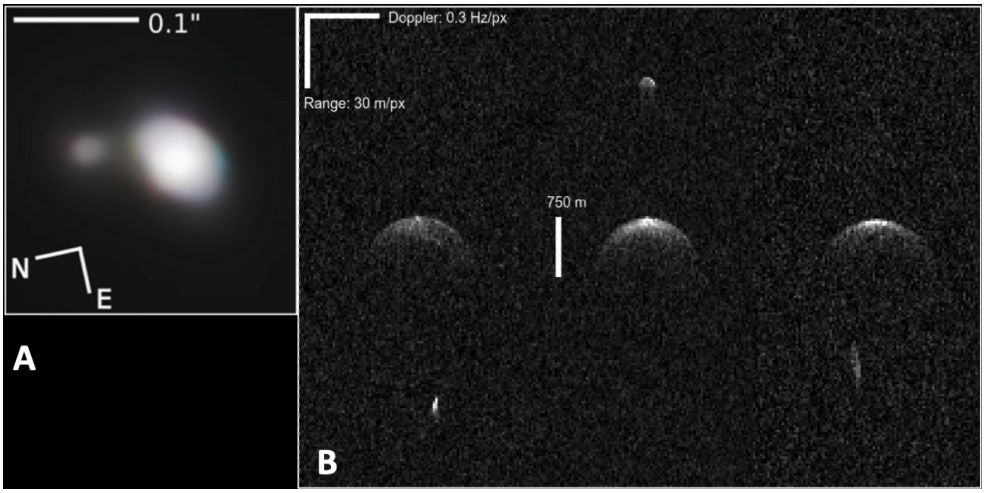

Figure 14. Binary NEA (66391) Moshup was observed by ground-based telescopes during a global planetary defense characterization exercise (Reddy et al. 2022a). A. The resolved image of the binary system was obtained with Very Large Telescope SPHERE instrument at 0.037 au. B. Arecibo radar delay-Doppler images with 30 m/px resolution at 0.05-0.07 au.

Stellar occultation studies of the solar system have proven over several decades their value in determining the size and shape of solar system bodies, as well as the derivation of high accuracy astrometry for asteroids. Elliot (1979) was already highlighting the potential of this method over 4 decades ago. Occultation campaigns typically involve multiple mobile telescopes equipped with fast cameras and high timing accuracy. They allow measurement of the apparent size of an object at the time of the occultation (Dunham et al. 2016) and constrain its position at that same epoch to a few milliarcsecond accuracy. Occultations can also allow the discovery of satellites, discovery and probing of rings around planets and small solar system objects, and even constraining the characteristics of atmospheres. Unlike radar measurements, occultations can probe an object regardless of its geocentric distance, from NEAs to trans-neptunian objects.

The first stellar occultation by an NEA was predicted nearly 48 years ago (Dunham 1974; Harrington et al. 1975). This was the occultation by the asteroid (433) Eros (16.8 km diameter) which belongs to the Amor dynamical population. This event of on January 24$^{\text{th}}$, 1975 was observable from New England. Several other occultations by Eros were observed over subsequent decades. Other occultations by NEAs (1036) Ganymed (37.7 km diameter) and (1685) Toro (3.4 km diameter) were recorded in the 1980s and early 2000s, respectively.

The 2021 encounter of Apophis with Earth has marked the beginning of a new era for occultations. Indeed, these were the first occultations by a sub-km sized object, and were made possible thanks to the high accuracy of the *Gaia* stellar catalogues which ensure an accuracy to the tenth of milliarcseconds (mas) for the stars (Gaia Collaboration et al. 2016, 2018, 2021). Furthermore, Apophis orbit was updated with 150 m precision range measurement a few days before the stellar occultation,

thus greatly improving its orbit. The successful Apophis occultations in March 2021 allowed a new position measurement to be derived with uncertainty of only ∼0.3 milliarcsec (mas), corresponding to 25 m at its distance, a measurement that compares with the Gaia quality level[3].

Several other occultations by Apophis were successfully observed in the following weeks and months. The success of these campaigns as well as most occultation campaigns is possible thanks to good predictions made possible by "good enough" astrometry and the ability to deploy several mobile stations thanks to the high commitment of amateurs and members of the IOTA (International Occultation Timing Association) across different continents.

The radar astrometry data in the line-of-sight direction and the occultation astrometry in the plane-of-sky are complementary to one another, while being similar in accuracy. However, Apophis will be in the daytime sky after the encounter, and thus during that time it will only be followed from the ground by radar.

We have nonetheless identified the first occultation opportunities starting in June 2029 (private communication with Josselin Desmars). We have listed these events in Table 5, and the associated maps can be found in Appendix B. We have chosen to present here only the opportunities between June 2029 and mid-October 2029; later occultation opportunities are as of yet too uncertain.

5.4. *Submillimeter Observations*

The mm/submm wavelength region has been used to passively observe thermal emission from planetary bodies, including asteroids. The depth to which observations are sensitive depends on both the thermal physical and dielectric properties of the regolith. Submillimeter observations of asteroids are typically used to determine the thermal properties within the top few millimeters of their regolith (Chamberlain et al. 2007).

The Atacama Large Millimeter Array (ALMA) is an interferometric array located at the Chajnantor site in Chile. It consists of fifty 12-m antennae, which can be moved relative to one another to allow for different spatial resolutions. ALMA is designed to measure passive thermal emission in the wavelength range from 0.3 mm to 3 mm (Busch 2009). ALMA has observed MBAs such as (1) Ceres (Li et al. 2020), (3) Juno (Hunter et al. 2015) and (16) Psyche (de Kleer et al. 2021; Shepard et al. 2021; Cambioni et al. 2022), as well as Jupiter Trojans (Simpson et al. 2022). ALMA has used been used to observe Centaurs and trans-Neptunian objects (Lellouch et al. 2017; Sheppard et al. 2018). These observations have primarily been used to constrain surface thermal inertia, often a proxy for regolith grain-size and/or porosity.

There are several constraints on ALMA that make observations of Apophis near its close approach time problematic or impossible: in particular, Apophis's northern declination and ALMA's slew rate limit are limiting factors. In addition, of course,

[3] https://www.cosmos.esa.int/web/gaia/iow_20210329

ALMA's position in Chile is not well placed for observations at the time of close approach in any case. However, windows exist on 12-13 and 14 April 2029 where observations can be made.

The ALMA configurations for 2029 have not been set, and so it is not yet known whether or not the Apophis will be resolvable or a point source. Given the typical weather in April, observations at 1 mm wavelength are favored over other wavelengths (Busch, personal communication). ALMA discourages observing blocks longer than 2 hours, which would preclude observations of a full rotational lightcurve for Apophis. However, if significant resurfacing events occur on Apophis during the Earth close approach, changes in Apophis's 1-mm emissivity prior to and after the close approach could potentially be measured from short-duration measurements.

There are many unknowns in these potential measurements and interpretations, however, since to this point no S-class NEOs have been measured at 1 mm. ALMA measurements of Didymos at the time of the DART impact are expected to be made, the results of which can be used to help design possible Apophis measurements in 2029.

Daytime observations can be made by ALMA to within a few degrees of the sun, which should allow observations of Apophis as it departs from the Earth encounter. Thermal emission observations of the "nightside" would be useful for thermal physical understanding if Apophis is sufficiently spatially resolved to differentiate between night and illuminated areas. If possible, this would be a unique observation that otherwise could only be accomplished with a rendezvous or orbiter spacecraft mission.

5.5. *JWST Observations*

JWST (Clampin 2008) is the most powerful spaceborne telescope available for characterization of Apophis. Motivations for its use include a full spectral characterization across the visible, near-, and mid-infrared for compositional studies, as well as measurement of its albedo. These measurements can plausibly be done prior to and after the Earth encounter, and from a different line of sight and phase angle than Earth-bound telescopes. JWST can also potentially provide very well calibrated data for comparison with any relevant spacecraft or telescopic data.

However, JWST observations are only possible for objects within a limited range of solar elongations (85 - 135°) and non-sidereal motions (< 30 milliarcseconds per second requirement, though higher rates may be offered after testing and in later cycles). Apophis violates the solar elongation limit until January 2028, but has four windows for observation within a year of close encounter: 18 January—21 March 2028, 16 December 2028—16 March 2029, 5 September—6 November 2029, and 5 January—18 March 2030. When including the current allowed maximum sky rate, the entire spring 2028 window is disallowed, but the other three windows remain valid

Table 2. Apophis science in 2029 enabled by ground-based and space-based optical facilities

Optical wavelength	Immediate data products	Apophis science	Example Facilities
IR	unresolved images	• effective diameter; • thermal inertia • limited mineralogy	NEO Surveyor
	spectra	• mineralogy and bulk composition; • space weathering; • taxonomy; • inferred microscopic surface density	SpeX@NASA IRTF
mm to sub-mm	unresolved? images	• thermal inertia	ALMA
Visible	lightcurves	• 3D convex shape model; • spin state; • moment of inertia ratios;	
	spectra	• taxonomy; • compositional analogs	ubiquitous
	occultation chords	• size; • limited shape information; • heliocentric orbit improvement	
	adaptive optics	• 10-m resolution images	SPHERE@VLT
	speckle imaging	• 10-m resolution images	QWSSI@LDT
	polarimetry	• regolith properties;• optical albedo;• surface heterogeneity	WIRC+Pol@Palomar 200”

NOTE—NASA IRTF - NASA Infrared Telescope Facility at Mauna Kea, Hawaii
ALMA - The Atacama Large Millimeter/submillimeter Array in the Atacama desert, northern Chile
VLT - ESO’s Very Large Telescope in Chile
LDT - Lowell Discovery Telescope, Arizona, USA
Palomar 200” - The Hale telescope at the Palomar Observatory, California, USA

in their entirety. For completeness, an increase in the tracking rate from 30 mas/s to 70 mas/s would allow the entire first window to be valid, and even an increase from 30 to 40 mas/s would allow 18 February—21 March 2028 to be within the tracking rates. Also, we note that even in situations where JWST cannot match the ideal tracking rate, observations may still be made at the maximum rate, with the target slipping across the field of view over a series of exposures. Finally, we note that the JPL Horizons system does not currently support calculation of ephemerides from JWST after 2024, so we assumed an observer on Earth in the discussion below.

JWST has four instruments allowing imaging and spectroscopy in the 0.6 — 28.8-μm region. The instruments all point to slightly different places, minimizing moving parts but also precluding simultaneous measurements with multiple instruments. The slews and overhead necessary for switching between instruments to view the same field of view are relatively modest, however, they still can amount to several minutes. The sensitivity of JWST makes saturation a risk for sufficiently-bright and warm targets (Rivkin et al. 2016; Thomas et al. 2016). The JWST Exposure Time Calculator (ETC) allows an estimate of the SNR and saturation likelihood of Apophis. We used the observing circumstances for the brightest time that it is within the solar elongation window, on 16 March 2029 when it is at V = 15.7, which sets the spectral energy distribution (SED) for Apophis for reflected light. Taking the NEOWISE measurements from (Satpathy et al. 2022) and adjusting for the different phase angle and distances from Earth and Sun between the NEOWISE measurement date and 16 March 2029, we estimate it will have a brightness of 100 μJy at 10 µm on the latter date. That brightness corresponds to an effective temperature of roughly 300-315 K. Forward calculations using literature values for Apophis' albedo and solar distance suggest it will have a subsolar temperature of 350-380 K on that date, depending upon the choice of beaming parameter.

Given these values, the NIRSPEC IFU saturates in PRISM mode between 0.7 — 2.25 μm at the minimum integration times, but provides good data from 2.25 — 5 μm and from 0.6 — 0.7 μm. Use of gratings with higher spectral resolution would allow unsaturated measurements across the entire 0.6 — 5-µm region with NIRSPEC, as would observations at a time when Apophis was fainter. Unsaturated measurements are available for MIRI with its Low Resolution Slit mode across its entire 5 — 13.8 μm range, with calculated SNR >> 1000 at most wavelengths < 13.1 μm. It is not clear that JWST imaging of Apophis would be useful, and initial use of the ETC suggests that unsaturated imaging might require observations when Apophis is fainter than maximum brightness and/or use of coronagraphic imaging (if searching for a dust cloud).

JWST observations are planned for the September 2022 DART impact into Dimorphos, at which time the Didymos system will be at a roughly similar brightness and phase angle as Apophis during the spring 2029 observing window, and moving at

much higher rates. We can expect the Didymos observations to help inform the best ways to use JWST's unique capabilities for observations of Apophis.

5.6. *Thermal-IR Imaging*

Thermal modeling of near-infrared observations is a powerful indirect technique to estimate asteroid sizes. Masiero et al. (2021) and the references within state that the the diameter uncertainty could be as good as 10% assuming that absolute magnitude H_V is known to within 0.2 mag. Thermal modeling of the near-infrared observations by NEOWISE suggests that the size of Apophis is 340 ± 70 m Satpathy et al. (2022), consistent with the radar estimate.

If the size and shape of an asteroid is already constrained, thermal physical modeling of infrared observations can be used to determine surface thermal inertia, which can be used to constrain grain sizes. MacLennan et al. (2022) demonstrated the approach for the active asteroid (3200) Phaethon. They found a difference in grain size between the northern and southern hemispheres.

Thermal emissivity spectra can provide information about composition. For example, spectra from 5-38 microns acquired using the Spitzer Space Telescope Infrared Spectograph (IRS) was used to determine that the Trojan asteroids (624) Hektor, (911) Agamemnon, and (1172) Aneas, likely have fine-grained silicates on the surface (Emery et al., 2006).

6. IN SITU OBSERVING OPPORTUNITIES

In situ experiments also provide a wide variety of possible observing methods that could yield insights from the close encounter. Although specific missions may be mentioned in this section in order to concretely illustrate the relevant capabilities, the SAT does not endorse or promote the use of any particular mission or instrument.

6.1. *Spacecraft Rendezvous*

The scientific return enabled by sending a spacecraft to asteroids has been demonstrated repeatedly. Observations at close range enable spatial resolution that is unachievable via remote observations. These high spatial resolution images open the possibility for the identification and study of surface features. For example, the Dawn mission's multi-band camera provided exquisite maps of the surface geology and composition permitting the identification of impact craters, landslides, and volcanos on Ceres and Vesta, while OSIRIS-REx at Bennu has identified particle ejections and produced detailed images of the rubble pile asteroid Bennu.

The majority of investigations into geophysical processes on asteroids enabled by spacecraft rendezvous have been forensic investigations, where detailed study of the observed structures and models of inferred physical processes have yielded insights about its history and the processes shaping its surface (e.g. Jawin et al. (2022), Delbo et al. (2022)). Despite the impressive amount of information resulting from these investigations, substantial uncertainties regarding the timescales and details of

the geophysical processes which shaped these asteroid's surfaces remain since those processes were not observed in action.

The close encounter of Apophis presents a unique opportunity to observe geophysical processes contemporaneously, rather than infer them after the fact. Multi-band optical-NIR, high spatial resolution maps before and after the Earth encounter would enable the identification of surface features that changed as a result of the encounter. Significant motions of larger rocks (decimeter to meter scale) or regolith displacement could be identified by comparing pre- and post- encounter images. If the surface motion involves motions of smaller rocks, then multi-band images could be used to identify changes in albedo, spectral slope, and/or spectral bands that result from the exposure of fresh, unweathered material. In the case of a clear detection of tidally induced resurfacing, combining the before and after surface morphology with models of the encounter would provide unprecedented insight into this geophysical process, essentially providing a ground-truth observation of the geophysical process of gravitationally induced tidal resurfacing.

Even in the case that no resurfacing on Apophis can be identified by comparing before and after high resolution multi-band images, substantial insights will be possible. A lack of identifiable resurfacing, when combined with topological information and the encounter geometry can be used to place lower limits on the surface cohesion.

In the low gravity regimes found on asteroids, cohesive forces may be the strongest ones experienced by particles. Interpretations of asteroid spin rates, in particular the maximum spin rate consistent with a rubble pile structure, is critically dependent upon understanding the cohesion of surfaces. Similarly cohesion is an important factor in the way that asteroid surfaces respond to disturbances, whether natural or caused by humans.

Furthermore, gravitational close encounters with planets is a leading model for how asteroid surfaces are refreshed. Statistical analyses comparing the orbits of resurfaced asteroids (e.g., Q types) and un-resurfaced asteroids are consistent with the thesis that gravitational close approaches within < 15 planetary radii cause resurfacing (Binzel et al. 2010), though other processes such as YORP may play an equally important role (Graves et al. 2018). If Apophis' ~ 6 Earth radii approach does not cause resurfacing, the role of gravitational interactions as a driver of asteroid resurfacing would need to be re-examined.

Another measurement that could be enabled by a spacecraft rendezvous would be to observe key portions of the Apophis' surface during the encounter. Existing models (e.g. Hirabayashi et al. (2021)) have identified the regions of Apophis that are most likely to experience higher levels of stress. A series of images taken at a rapid cadence monitoring these regions throughout the encounter would provide a real-time view of geophysics in action. Imaging during close encounter could observe other transient events such as pebbles being ejected (due to landslides, lofting, or some other mechanism) during the hours around close approach. OSIRIS-ReX has ob-

served this phenomenon at Bennu, albeit the root cause of the asteroid activity was different. Chesley et al. (2020) showed that observations of the ejected particles could be highly valuable; their trajectories enabled to derive Bennu's gravitational coefficients through degree 8 and to resolve nonuniform mass distribution through degree 3.

High resolution multi-band imaging of Apophis from only one epoch (either pre- or post- encounter) would provide a wealth of information about the asteroid, similar to what has been learned about Bennu, Ryugu, and other spacecraft targets. However, single epoch observations, even of the post-encounter observations would only enable forensic investigations of the geophysics. Given the relatively long timescale of space weathering, the epoch of any resurfacing identified in post-encounter only images would be ambiguous. Without knowing that identified areas of resurfacing were caused by the 2029 encounter, modeling of these regions would not be able to be linked uniquely to the geometry of the 2029 close encounter.

6.2. *Spacecraft Flyby*

Flyby missions are typically less constrained in mission design than rendezvous missions. This has led to the recognition in the planetary defense community that they may be well suited to rapid characterization of hazardous objects, returning knowledge about key physical parameters that is sufficient to begin planning for deflecting a particular object. Previously executed spacecraft flybys have successfully produced detailed images of the surfaces of asteroids (e.g. Huang et al. (2013) and Barucci et al. (2015)). While these maps are generally confined to a subset of the asteroid's surface, they have nonetheless been sufficient to investigate cratering history (Marchi et al. (2010)), identify landslides (Schröder et al. (2010)), and diagnose space weathering (Schröder et al. (2015)).

The pre- and post- encounter observations required for the contemporaneous investigation of geophysical processes discussed in §6.1 do not necessarily have to be performed by a single spacecraft. Either the pre- or post- or both sets of images could be obtained by a well timed flyby mission. The regions most likely to experience resurfacing have been identified by current models (e.g. Hirabayashi et al. (2021)). When coupled with detailed information about the spin state, a flyby could be timed such that the regions most likely to experience resurfacing would be imaged by the spacecraft, preferably at low phase angle. The pre- and post- flyby images would likely to be obtained at slightly different flyby geometries, under different lighting conditions, and possibly with cameras with different specifications. Thus, it would be necessary to do detailed topographic surface reconstruction in order to be sure that the changes are real. While combining data from two separate spacecraft would undoubtedly present challenges, this approach would enable an unprecedented investigation of the geophysical process of tidal resurfacing.

6.3. *In situ seismometers*

The use of in situ seismometers on the surface of both Earth and Mars have been used to detect asteroid impacts as well as provide invaluable information related to the planetary bodies interior structure. For terrestrial applications, modern seismometers can measure displacements as small as 1 nanometer. The state of the art seismometer operating on another planetary body's surface is the Mars InSIGHT Seismic Experiment for Internal Structure (SEIS) instrument. The Apollo and InSight seimic experiments are currently the gold standard for accuracy at $10^{-10} m/s^2/\sqrt{Hz}$ (Mimoun et al., 2021). For perspective, measuring the tidal forces on the martian moon Phobos where tidal acceleraions are expected to be approximately 0.57 mm/s^2 would require instrumental noise levels to be less than 5.4 $10^{-9} m/s^2/\sqrt{Hz}$ (Bernauer et al. 2020). Small seismometers, with size, weight, and power (SWaP) specifications suitable for deployment to the surfaces of NEAs are currently under development (e.g., Murdoch et al., 2021)

The performance of seismometers on the surfaces of small bodies may have less accuracy if not properly coupled to the ground. While a non-coupled seismometer may still be useful to monitor local landslides or regolith shifts, its utility for measuring seismic waves, and thus internal structure, may be quite limited (Sava & Asphaug, 2019). Sava & Asphaug (2019) have suggested laser doppler vibrometry as an alternate to in situ seismic sensors. Because Doppler shifts only record displacements in the in-line direction, multiple laser doppler vibrometers (LDV) would be needed to monitor surface translations. Sava & Asphaug (2019) recently investigated the use of LDV for a seismological study of small solar system objects, leading the way to the possibility of high-resolution imaging a small body's mechanical interior.

Probing asteroids' interiors has been a challenge tackled by the community since the late 1970s, with the first projects to a mission to NEAs (French & Hulkower 1982) and the project for the AMBASSADOR (A Main Belt Asteroid Seismic study and Sample Acquisition to Determine meteorite ORigins) mission to S-class asteroid (7) Iris (Turtle et al. 1999). While Binzel et al. (2003) present a detailed overview of the foundations and perspectives in terms of studying the interior of small solar system object; they state "Taking further steps toward directly studying small body interiors will require applying the tools of modern geophysical prospecting: radar reflection and transmission tomography, seismo-acoustic waveform inversion, magneto-telluric imaging, and good old-fashioned drilling and blasting" . The latter is obviously not an option in the case of Apophis. The challenges described in this paper are still true nearly 20 years later, and even more in the case of Apophis.

For Apophis, in situ seismic measurements, where the instruments are firmly coupled to the surface, could be an order of magnitude more sensitive to potential vibrations and accelerations than remote sensing techniques and allow for the possibility of multiple monitoring sites, which may be necessary of the detectors are mostly sensitive to local displacements. Because the expected level of surface disruption is expected to be small, this level of sensitivity may be needed to fully characterize the effects

from close approach. In addition, because the changes are expected to occur over a short duration (< 1 hour), continuous in situ measurements will also have greater reliability to monitor the entire event at high sampling frequency.

7. OPPORTUNITIES AND RECOMMENDATIONS

As discussed above, the close approach of Apophis provides a unique opportunity to observe the interaction of an asteroid with a planet in real time and to utilize a wide variety of observing techniques to monitor the event. The Terms of Reference for the Specific Action Team requested a prioritization of the opportunities presented by the close approach. In order to determine priorities, the SAT evaluated whether the opportunity capitalized on the unique physical processes of the close approach, the value to planetary science and planetary defense to likely outcomes of the investigation, and the readiness of the required technologies. While there are numerous observational opportunities that are likely to yield impactful science results, two highly compelling and unique opportunities were identified: *(i)* to directly monitor geophysical processes in real time using high resolution multi-band near-ir imaging and *(ii)* to probe the interior mass distribution based on the NPA spin state and encounter dynamics

Additional compelling, though not top priority, opportunities are also discussed. Finally, in order to fully capitalize on the Apophis close approach, it is important to prepare and practice for the Apophis close approach.

7.1. *Top priority opportunities*

7.1.1. *Direct Observations of Geophysical Processes*

The surfaces of asteroids are the result of a variety of geophysical processes including collisions, thermal fracturing, tidal interactions, space weathering, accretion, and electrostatic lofting. Understanding these processes and their interplay is essential in order to connect the observable face of asteroids to their history and role in the formation and evolution of the solar system. However, the vast majority of our knowledge about these processes relies on modeling the outcome of these processes and comparing those models to observations. In other words, we have inferred the actions of these processes - but have rarely had the opportunity to observe any of these geophysical processes in action. The close encounter of Apophis provides a unique chance to witness geophysical modification of an asteroid's surface as it happens. There are two geophysical processes which may be observable during the Apophis close encounter: resurfacing due to tidal interactions and particle lofting due to electrostatic or tidal forces. Our understanding of both of these processes have outstanding uncertainties. Observations targeting the investigation of tidally driven resurfacing was identified as a top priority opportunity.

The potential effects of tidal interactions have been modeled by several teams (see §4.3). The size of the predicted effects vary widely from little to no motion of surface material (e.g. Yu et al. (2014), DeMartini et al. (2021) Scheeres et al. (2020)), up to movement of meter-scale surface boulders(e.g. DeMartini et al. (2021)). While there

are differences in these predictions due to the modeling approach, in most studies, the amount of motion predicted depends on the geometry of the close approach, local topography, and cohesion. Any detection of motion of surface material would allow real time observations of this geophysical process, resulting in refinements of models and estimates of the strength of cohesion. A non-detection would provide a lower limit on the cohesive strength. Either result would provide significant insights into the role of tidal effects on the resurfacing of asteroids.

One or more spacecraft with a high resolution, multi-band optical-NIR imager in close proximity to Apophis before and after the close encounter would be sufficient to make direct observations of this effect. Monitoring during the event would be highly informative, but not required to enable the identification and study of tidally induced resurfacing. If tidally induced surface motion involves significant movement of larger rocks (decimeter to meter scale), comparisons of the images prior to and after the encounter could be used to directly identify the altered regions. If the surface motion involves small motions or smaller rocks, then the multi-band images could be used to identify changes in albedo, spectral slope, and/or spectral bands that result from the exposure of fresh, unweathered material. More details about this opportunity are discussed in §6.1 and §6.2.

There are other observing methods which might allow an inference of surface movement. If it were of sufficient scale, remote observations (e.g. changes in surface features in high-resolution delay-Dopper images, changes in radar polarimetry parameters, multi-band speckle imaging, vis-NIR spectroscopy) may allow an inference of surface movement. If an in-situ seismometer was placed near the region of resurfacing and was sufficiently coupled to the surface, a signal might be detected. But only the combination of pre- and post- encounter images from a spacecraft can provide a direct measurement if resurfacing occurs. Furthermore, if resurfacing is not detected, images from a spacecraft will enable a lower limit on the cohesive strength.

7.1.2. *Internal mass distribution*

The interior structure of NEAs is of significant interest to both planetary science and planetary defense. We currently have information about the interior structure of only a small handful of NEAs (a subset of the spacecraft targets). For planetary science, the interior structure of an asteroid carries the imprint of the body's collisional and accretion history, and is therefore a window into the evolution of the inner solar system. For planetary defense, the interior structure of an asteroid is one of the major sources of uncertainty in how it would react during atmospheric entry and how it would respond to mitigation attempts.

The non-principal axis rotation of Apophis enables an investigation of the asteroid's interior by comparing the moments of inertia ratios derived from the dynamics and shape. If the asteroid spins like a uniform density body, the dynamical inertia tensor will only have the diagonal components that match the shape values.

We already have very strong constraints on Apophis's pre-flyby spin state thanks to the extensive optical lightcurves observations in 2012/2013 and 2020/2021 (Pravec et al. 2014; Lee et al. 2022). This will only get better with the addition of more optical and radar data during the 2029 event.

Radar will be able to fully map the spin state (3 Euler angles, 3 body rates, 2 ratios of moments of inertia) of Apophis both pre and post flyby. (See §5.2 for more details.) Optical lightcurves will be able to do the same for the pre-flyby spin state and then several months after the flyby during the late 2029 observing window.

The modification of the spin state during the close approach depends on the initial orientation, the distribution of mass within the asteroid, and possibly tidally induced material movement. Modeling of the observed initial and final spin states will provide additional constraints about how uniform the mass distribution is within the asteroid, provide limits on the amount of material that shifted during the encounter, and constraints on the strength of the asteroid.

7.2. *Other opportunities*

In addition to the investigations discussed above, the Apophis close approach will enable a variety of additional opportunities. Below are several intriguing possibilities, but there was insufficient information available for an evaluation of these investigations. Subsequent research could illuminate the potential of these studies.

Lofting of Material: A variety of processes can loft particles off of the surface of asteroids, including rotational disruption, sublimation, meteoroid impacts, thermal stress fracturing, tidal stresses, and electrostatic lofting. Two of these processes may be observable during the Apophis close approach. Particles may be levitated from the surface as the result of resurfacing or electrostatic lofting. In either case, the detection of newly lofted material would provide new insights into these geophysical processes and the surface properties of Apophis. The detection of material levitated during a tidal stress induced resurfacing event would be complementary to observations of surface motion, providing insight into the tidal stresses and the cohesive strength of Apophis's regolith.

Electrostatic lofting occurs when the electrostatic force acting to detach a particle from the surface is larger than the gravity and the cohesion that bind the particle to the surface. It has been hypothesized to occur on the moon (Rennilson & Criswell 1974) and asteroids (Lee 1996). An analysis by Hsu et al. (2022) concluded that electrostatic removal of fine-grained regolith may dominate production mechanisms, resulting in the loss of fine regolith on sub-km asteroids. The size distribution of regolith is likely to affect the thermal inertia (and as a result the Yarkovsky drift) and reflectance spectra of asteroids, so understanding the process of electrostatic lofting has implications for both planetary defense and planetary science.

Like many other geophysical planetary processes, there is limited data which permits observing this process in action. Recently, Hartzell et al. (2022) assessed whether electrostatic lofting could explain the ejected particles observed at Bennu (Lauretta et al. 2019) and concluded that while submillimeter particles could feasibly be electrostatically lofted from Bennu, the size and speed of the observed particles were inconsistent with electrostatic lofting.

Apophis's close approach could provide a unique experiment for the electrostatic lofting process. During Apophis's close approach, because of passage through the Earth's magnetotail and the outer Van Allen Belt, the asteroid will experience a larger flux of high energy electrons than usual and experience an increased charging of particles which may in turn mean that more particles get lofted than usual. The detection of electrostatically lofted particles in this unique scenario would provide an unprecedented test of this process. A null result, when coupled with observations of the particle size distribution on the surface, would provide limits on cohesion and provide insight into the effectiveness of electrostatic lofting. Unfortunately, to date there are no studies in the literature which have investigated the electrostatic lofting of particles during the close approach of Apophis. Absent such a study the SAT could not place this opportunity in the top priority category, however does suggest this is an intriguing opportunity deserving of study.

In-situ seismometry: The close encounter with Earth will impart tidal energy to Apophis that will be transmitted and dissipated as seismic waves in its interior. This may cause a change in the shape of Apophis. Regardless of whether this energy input results in shape deformation and/or the movement of surface material, it would be valuable to measure these seismic waves. Additional feasibility studies need to determine if in situ seismometers can be sufficiently coupled to the surface to achieve better performance than remote sensing techniques, such as laser vibrometry. Regardless of the technique, if detected, this would provide a rare view into gravity-induced reshaping and could provide insights about Apophis's interior structure and strength.

Structure of Top $\sim$ 10's of meters: The close approach of Apophis opens up the possibility of using long wavelength radar from the ground to probe the structure of the surface down to tens of meters, depending on the wavelength. (For example, 100MHz wavelength radar could penetrate 30m into the surface.) This would provide additional insights into the internal structure of the asteroid and would be complementary to the opportunity discussed in §7.1.2.

7.3. *Coordination, Readiness, and Practice Campaigns*

For singular events like the 2029 Apophis flyby, there is a strong need for coordinating observations and establishing preparedness across a wide range of facilities/capabilities. Furthermore, many of the potential science investigations would

Table 3. NEA close approaches 2027-2029

Asteroid	Date	Geocentric Distance	Object's size	Peak app. H	Peak ang. rate
		LD	m	mag	arcsec per min.
(137108) 1999 AN10	2027-Aug-07	1.0	650−1000	7.5	∼830
(153814) 2001 WN5	2028-Jun-26	0.6	932±11	6.8	∼510
2011 LJ19	2028-Jul-25	3.3	150−330	15.0	∼95
(35396) 1997 XF11	2028-Oct-26	2.4	704±103	8.6	∼185
(292220) 2006 SU49	2029-Jan-28	3.2	330−750	13.3	∼50
(99942) Apophis	2029-Apr-13	0.1	340±40	3.2	∼2400
2001 AV43	2029-Nov-11	0.8	32-71	15.1	∼160

NOTE—The nominal close approach distance to Earth is expressed in lunar distances. One lunar distance is equivalent to 380,000 km. The orbit of 2011 LJ19 still contains large uncertainties, although we know that it will not approach closer than 0.7 LD.

benefit from timely sharing of results to enable detailed analyses of the event. Previous campaigns that focused on near-Earth encounters highlight the need for redundancy in instrumentation to ensure that opportunities to collect critical data are not missed due to bad weather or a given facility going offline (Reddy et al. 2019, 2022a,b).

For Apophis there will be unique observational challenges (Figure 11): the non-sidereal rates will be orders of magnitude higher than an average NEO and the brightness of Apophis will make image saturation an issue in the optical/NIR, particularly for large aperture facilities. This last challenge is also an opportunity because such a bright target enables a wide variety of characterization techniques, some of which are not possible (e.g. speckle imaging) for typically faint NEOs. To address these potential issues it will be important for observers to test and validate their systems. Artificial satellites can serve as good analogs to Apophis in terms of brightness and non-sidereal motion. However, there are also several known NEOs that can serve as practice targets when they experience near-Earth encounters in the years leading up to 2029.

Figure 3 shows currently known NEAs that will make less than five lunar distances approach within the next ten years. Table 3 shows details for the seven largest objects. Observing campaigns for these close approaches would provide excellent rehearsals for the Apophis close approach and are also likely to yield interesting science results.

All NEAs listed in Table 3 will be exceptionally strong radar targets, and given how little is known about these objects at the moment, we will have excellent opportunities for scientific discoveries. They will also provide an excellent "target practice" for facilities that have little or no experience of observing NEAs. Furthermore, experimental

and less mainstream techniques, such as interior sounding with long wavelengths ground-based radars (Haynes et al. 2022), speckle imaging, and polarimetry will have a chance for a proof-of-concept and to make unique contributions.

An additional area requiring coordination is to ensure that radar observations can proceed even if there are spacecraft operating near Apophis during the close approach. X-band (8560 MHz) and S-band (2380 MHz) frequency radars have illuminated spacecraft before, with no issues reported by the mission teams. However, some radars operate in C-band (7190 MHZ), and this frequency is known for spacecraft communication. It is not clear if radar observations would cause any interference issues for a spacecraft that happens to be in the vicinity of Apophis. C-band klystrons are the ones that enable 1.875 m resolution imaging, so these radar facilities would likely be operating in the days around the close approach in order to produce high-resolution imaging. As such, we should have a robust plan for any potential spacecraft operations during radar observations (and vice versa).

8. HAZARD ASSESSMENT FOR SPACECRAFT CONTACTS WITH APOPHIS

This section benefited from extensive discussion and analysis by Davide Farnocchia of the Center for NEO Studies at NASA's Jet Propulsion Laboratory.

8.1. *Background*

In this section we address the question of what kinds of spacecraft interactions with Apophis can be considered safe for Earth, in light of the asteroid's history as a potential impactor. The obvious concern is whether or not a change in orbit due to some kind of spacecraft contact can move Apophis from its currently safe orbit back onto a threatening orbit (Farnocchia & Chesley 2022).

The question is somewhat poorly posed given that we do not know in advance when any hypothetical spacecraft interaction would occur, nor the magnitude or direction of the effective change in velocity ΔV. Indeed, without some boundaries, we cannot even say in which year a new potential impact may fall. To make the problem tractable, we shall assume that any ΔV is to be applied within five years of the April 2029 Earth encounter, thus in the interval April 2024–April 2034. We also consider only potential Earth impacts within 100 years from present.

To further limit the range of cases to be studied we will consider only two values of ΔV. The larger of these is derived from a fictitious kinetic impactor (KI) mission with a 2000 kg spacecraft impacting Apophis at a relative velocity of 20 km/s. Neglecting momentum transfer due to ejecta and assuming an asteroid mass of 4×10^{10} kg, this leads to $\Delta V_{\rm KI} = 1$ mm/s.

The other ΔV that we consider serves as an upper bound on the orbital perturbation from a science mission. Here we consider a 40 kg SmallSat launched onto a geocentric orbit that impacts Apophis by maneuvering so that it is in the asteroid's path during the 2029 encounter. Given the Apophis flyby velocity at perigee of 7.4 km/s this leads to a $\Delta V_{\rm Sci} = 7$ μm/s. This is a strong upper bound for a science investigation. As

an example, a touch-and-go sample collection for which there is 50 N of force acting on the asteroid for 5 s, similar to the OSIRIS-REx contact with Bennu (Ballouz et al. 2021), would yield a ΔV more than three orders of magnitude below our $\Delta V_{\rm Sci}$. Moreover, the soft landing (at 25 cm/s) of our 40 kg SmallSat would be a factor 25 less than our hypothetical sample collection event. As a final example, a low speed flyby of a 1 ton spacecraft (at 1 m/s and 500 m periapsis distance) would lead to a ΔV that is similar to our SmallSat lander example. The possibility of an accidental spacecraft impact on Apophis should be analyzed separately as a part of mission development, especially for flyby missions, where the accidentally imparted ΔV would likely exceed $\Delta V_{\rm Sci}$.

While we only consider the two values $\Delta V_{\rm KI}$ and $\Delta V_{\rm Sci}$ for the deflection, we do not restrict the direction that the ΔV can be applied. Moreover, we allow the epoch of the deflection to be anywhere in a ten-year interval centered on the 2029 Earth encounter.

As a point of departure, we note that on its present trajectory Apophis cannot reach Earth for at least the next 100 years (Farnocchia & Chesley 2022, see also https://go.nasa.gov/3vLmpqI). Even so, there will be eight Earth encounters within 0.1 au during the next century, starting with the extraordinary approach in 2029. Table 4 details the circumstances of these close approaches, each of which will be considered individually. We note that radar observations will be possible for all listed apparitions, assuming current capabilities.

Table 4. Close encounters of Apophis with Earth within the next 100 years. Only encounters closer than 0.1 au are shown.

	3σ Time Uncert.	Distance (au)	
Date & Time	(HH:MM)	Nominal	3σ Minimum
2029-Apr-13 21:46	$<$ 00:01	0.00025	0.00025
2044-Aug-24 06:50	21:08	0.08033	0.07895
2051-Apr-20 01:55	08:24	0.04146	0.03981
2066-Sep-16 02:10	08:36	0.06956	0.06352
2080-May-09 08:16	13:38	0.08693	0.08602
2087-Apr-07 12:15	03:54	0.09581	0.09361
2102-Sep-11 20:32	15:55	0.02343	0.02249
2116-Apr-12 17:50	7.6 days	0.01946	0.00101

SOURCE: JPL Solution 216. Additional close approach information, including encounter animations, can be obtained at https://cneos.jpl.nasa.gov/ca/.

8.2. *Analysis Framework*

Impact hazard analyses can be conveniently conducted in the b-plane framework. The b-plane is oriented orthogonal to the inbound asymptote of an asteroid's hyperbolic orbit, with the geocenter at the origin. The intersection of the inbound

asymptote with the b-plane is denoted by $\vec{b}$, a vector in the b-plane, with $b = |\vec{b}|$. Roughly, one can think of the b-plane as the view the asteroid sees as it approaches the Earth, with $\vec{b}$ locating the asteroid's aim point. If the aim point is within the Earth *capture cross-section* then an impact will occur. The capture cross-section is defined by $b < b_\oplus$, where $b_\oplus$ is somewhat larger than the planet radius due to gravitational focusing. For Apophis, $b_\oplus$ is about 2.2 Earth radii, although that can vary by a factor of ∼1.4, depending on the encounter velocity of the close approach under consideration. (See, e.g., Farnocchia et al. (2019) and references therein for a complete development of the b-plane theory.)

The typical impact hazard analysis approach looks at the location of the predicted value of $\vec{b}$, as well as the prediction uncertainty, which can often be adequately approximated by a confidence ellipse centered at $\vec{b}$. If the ellipse overlaps the Earth then an impact is possible and the impact probability can be calculated by integrating the probability density over the capture cross-section. In practice, the confidence ellipse is often extremely narrow in relation to its length, and so can appear as a line in plots.

Our approach here is to model a change in velocity in an unknown direction by increasing the velocity uncertainty at the deflection epoch and mapping this uncertainty forward to the b-plane of the encounter in question. Specifically, we add the square of ΔV to each the diagonal elements of the velocity covariance at the deflection epoch. This leads in a natural way to an enlarged b-plane ellipse reflective (at 1-sigma) of applying the given ΔV in all directions. If the enlarged b-plane ellipse does not overlap the Earth then the application of the given ΔV (in any direction) at the assumed deflection epoch cannot lead to an impact.

The action of the Yarkovsky effect—and its uncertainty—is fully accounted for in the following analysis. Of particular note, there is the possibility that the rotation state of Apophis could change as a result of tidal forces during the 2029 encounter (e.g. Scheeres et al. (2005)), which would lead to a change in the Yarkovsky drift rate after 2029. However, this manifests only as a small shift (up to ∼500 m) in the b-plane location of the impact keyholes in 2029 and does not materially change the impact probabilities associated with a given keyhole (Farnocchia et al. 2013).

8.3. *Results*

As an opening example, we consider first the 2044 encounter of Apophis, starting with a hypothetical deflection 5 years before the Apophis encounter with Earth. Figure 15 shows the effect of such a ΔV for both $\Delta V_{\rm Sci}$ and $\Delta V_{\rm KI}$. From the figure it is clear that the b-plane ellipses do not overlap the Earth, and therefore an impact cannot take place for any $\Delta V < \Delta V_{\rm KI}$. Even so, the early defection with $\Delta V_{\rm KI}$ leads to a dramatic increase in the extent of the uncertainty ellipse, so that the uncertainty in the long axis exceeds the miss distance.

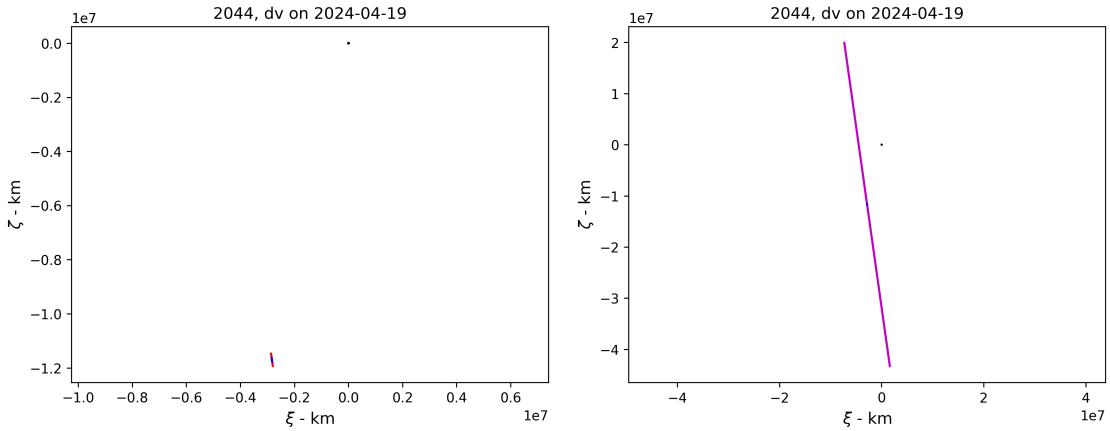

Figure 15. The Apophis 2044 b-plane with deflection taking place at 2024-Apr-19 with $\Delta V_{\rm Sci} = 7$ μm/s (left) and $\Delta V_{\rm KI} = 1$ mm/s (right). The geocenter is marked by the dot at the origin. The small blue segment at the center of the red ($\Delta V_{\rm Sci}$) or magenta ($\Delta V_{\rm KI}$) ellipse represents the encounter uncertainty if no ΔV takes place.

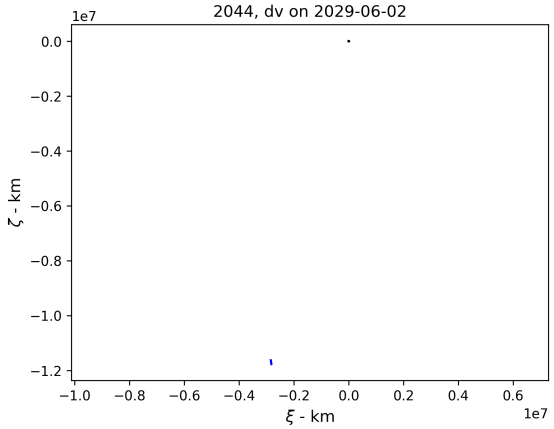

Figure 16. The 2044 b-plane with $\Delta V_{\rm KI}$ taking place 2029-Jun-02, several weeks after the Apophis encounter with Earth. The depiction follows the same scheme as that of Fig. 15, but in this case the deflection ellipse is negligibly larger than the no-deflection ellipse, and so only the no-deflection ellipse is visible. The plots with $\Delta V_{\rm Sci}$ and $\Delta V_{\rm KI}$ are indistinguishable.

Looking instead at the case where the deflection is affected *after* the 2029 Earth encounter, Fig. 16 reveals that even the larger $\Delta V_{\rm KI}$ is not large enough to significantly affect the 2044 encounter uncertainty. This is because the no-deflection uncertainty alone is significantly larger than the post-encounter ΔV.

Considering now the full 10-year range of candidate deflections and their effect in 2044, we see in Fig. 17 that the uncertainties associated with deflections less than $\Delta V_{\rm Sci}$ are always below the undeflected encounter distance and therefore an impact is not possible. On the other hand, the uncertainty from deflections with $\Delta V_{\rm KI}$ do exceed the encounter distance if taking place before early 2027. This is a necessary

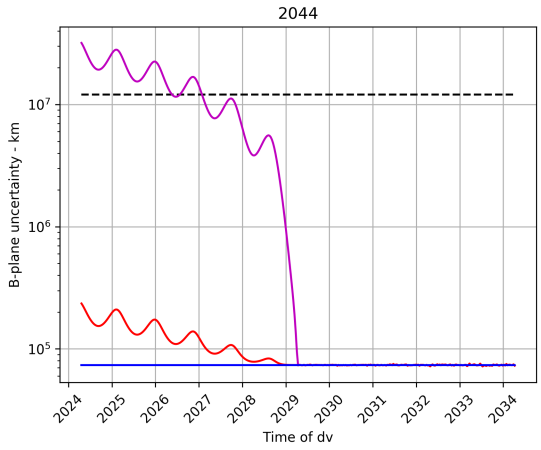

Figure 17. The Apophis b-plane uncertainty at the 2044 Earth encounter as a function of the time that a deflection is applied. The blue curve indicates the uncertainty with no deflection, the red curve reflects a deflection of magnitude $\Delta V_{\rm Sci}$, and the magenta curve a defection of $\Delta V_{\rm KI}$. The dashed black line marks the actual miss distance b.

but not sufficient condition for a deflection to lead to an impact, and as we have seen in Figure 15, the 2044 impact is not possible, despite the large b-plane uncertainty.

We turn now to the other encounters listed in Table 4, except 2044, which we have already considered, and 2116, which is a more difficult case that we analyze in the next section. Figure 18 shows the Apophis uncertainty at six Earth encounters as a function of deflection epoch in the same manner as Fig. 17. From these plots it is clear that a deflection of magnitude less than $\Delta V_{\rm Sci}$ at any time in our 10-year interval cannot lead to an impact at the respective encounters. However, with the exception of 2029, an impact cannot be ruled out on the basis of Fig. 18 for deflections of $\Delta V_{\rm KI}$ that take place before the Apophis encounter with Earth in 2029. For these cases a more detailed analysis is required, and the simple analysis used to rule out the 2044 impact may be insufficient. This is because the separation between the uncertainty ellipse and the Earth can be small enough that nonlinear effects must be considered, invalidating the linear assumptions employed here. Moreover, for $\Delta V_{\rm KI}$ applied before 2029, the possibility of strong interactions with Earth at one of the years that are considered here could lead to new and potentially threatening encounters during other years that are not considered here.

8.4. *Extended Analysis for 2116 and Subsequent Encounters*

The situation with the Apophis encounter with Earth in 2116 is less straightforward than the earlier encounters. This is because a very deep close approach is already possible for the undeflected trajectory. In Table 4 the first seven entries have minimum encounter distances that are similar to the nominal encounter distance, but for 2116 this is not the case. The nominal encounter distance in 2116 is ∼0.02 au, while the minimum is ∼0.001 au, less than half the lunar distance. Indeed, the uncertainty for even the undeflected orbit exceeds the nominal miss distance (Fig. 19).

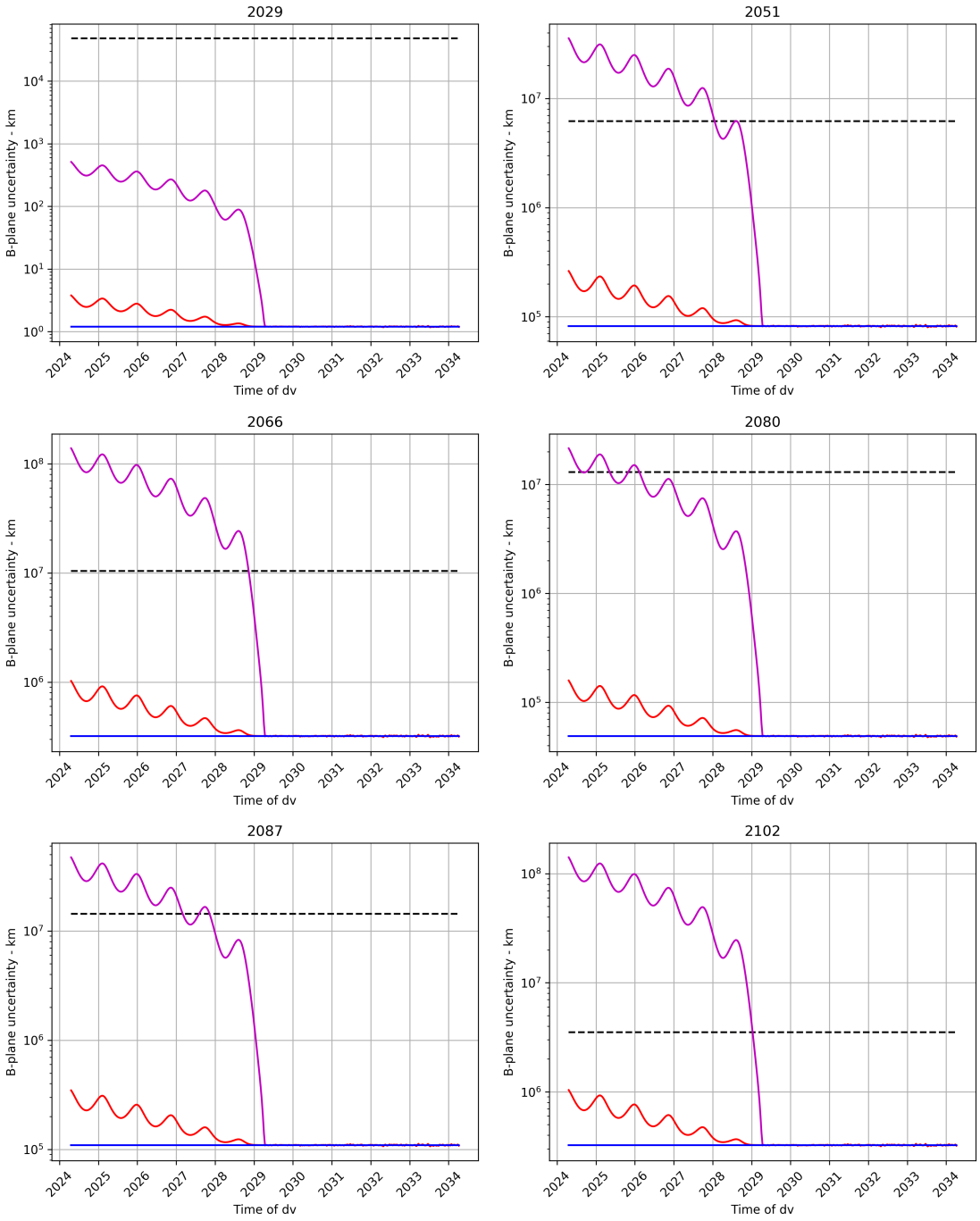

Figure 18. The same presentation as Fig. 17, but for Earth encounters in 2029, 2051, 2066, 2080, 2087, and 2102.

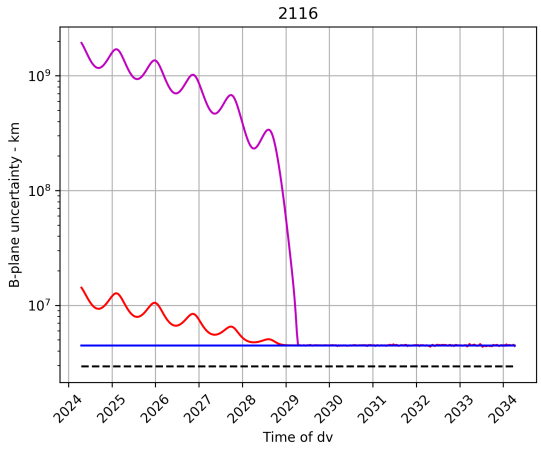

Figure 19. The same presentation as Fig. 17, but for the Earth encounters in 2116.

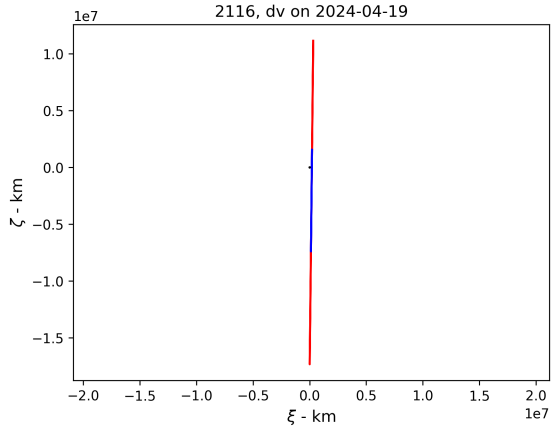

Figure 20. The Apophis 2116 b-plane with deflection taking place at 2024-Apr-19 with $\Delta V_{\rm Sci}$. The geocenter is marked by a dot at the origin. The blue segment at the center of the red ellipse represents the encounter uncertainty of the undeflected trajectory.

This characteristic is evident from Fig. 20, which depicts the undeflected encounter uncertainty ellipse in 2116 (in blue) and the corresponding uncertainty (in red) for a deflection of magnitude $\Delta V_{\rm Sci}$ taking place in 5 years before the Earth encounter. The no-deflection ellipse is already close to the Earth (at a distance of $\sim$0.001 au, according to Table 4) near its tip, while the $\Delta V_{\rm Sci}$ deflection roughly triples the extent of the uncertainty ellipse. Though it cannot be seen at the scale of the plots, a careful analysis shows that both the deflected and undeflected ellipses in Fig. 20 are well clear of Earth. Similarly, from Fig. 21, it is clear that deflections as great as $\Delta V_{\rm KI}$ after April 2029 cannot lead to impact in 2116.

The conclusion from Figs. 19–21 is that deflections within our parameters cannot lead to an impact in 2116. However, the possibility of sub-lunar-distance encounters in 2116 poses the possibility of strongly nonlinear outcomes in the years after 2116. In the parlance of hazard assessments, we have a "keyhole" problem in 2116, and

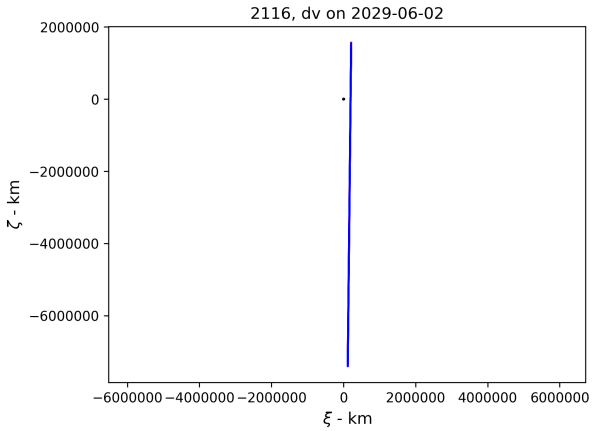

Figure 21. The 2116 b-plane with $\Delta V_{\rm KI}$ taking place 02-Jun-2029, several weeks after the Apophis encounter with Earth. The depiction follows the same scheme as that of Fig. 15, but in this case the deflection ellipse is negligibly larger than the no-deflection ellipse, and so only the no-deflection ellipse is visible. The plots with $\Delta V_{\rm Sci}$ and $\Delta V_{\rm KI}$ are indistinguishable.

there is the possibility of close Earth encounters in nearly every year starting from 2022. Our approach to resolving this problem is the simple, brute-force approach of Monte Carlo. In this scenario, the scattering effect of the possible deep encounter in 2116 overwhelms any possible $\Delta V_{\rm Sci}$ deflection attempt, and there is little need to include the deflection in the Monte Carlo. Even so, our Monte Carlo runs included a deflection of magnitude $\Delta V_{\rm Sci}$ on 2024-Sep-16 and in an arbitrary direction. Our Monte Carlo samples were taken at the epoch of deflection and included uncertainties in the Cartesian state as well as the Yarkovsky acceleration. In 10^7 Monte Carlo samples we found no impacts through 2150. Leveraging Poisson statistics, we conclude with 99% confidence that the probability of impact in any of the years from 2116–2150 is below 5×10^{-7}.

8.5. *Summary*

The foregoing analysis shows that the slight deflection associated with a science investigation of Apophis will not cause Apophis to impact Earth within 100 years from present. For this, we assume a $\Delta V < 7$ μm/s taking place within 5 years before or after the April 2029 encounter between Apophis and Earth.

On the other hand, the situation is more subtle for larger deflections that may be associated with a kinetic energy deflection demonstration. Here we assume deflections up to 1 mm/s and we find that such deflections are assuredly safe only if applied after the Apophis encounter with Earth in April 2029. Deflections of such magnitude applied *before* April 2029 will greatly increase the spread of possible trajectories of Apophis after the 2029 encounter and thus require a detailed analysis (beyond the scope of this report) that takes into account the direction of the planned deflection and fully accounts for nonlinearities in the mapping from the defection epoch to subsequent encounters.

ACKNOWLEDGMENTS

The Apophis SAT has benefitted significantly from conversations with and personnel communications from several subject matter experts including Lance Benner, Michael Busch, Christine Hartzell, and Josselin Desmars. In particular, the Apophis SAT would like to acknowledge extensive support from Davide Farnocchia (Jet Propulsion Laboratory) in the preparation of Section 8. A portion of this work was conducted at the Jet Propulsion Laboratory, California Institute of Technology, under a contract with the National Aeronautics and Space Administration (80NM0018D0004).

REFERENCES

Acton, C., Bachman, N., Semenov, B., & Wright, E. 2018, Planet. Space Sci., 150, 9, doi: 10.1016/j.pss.2017.02.013

Ballouz, R. L., Walsh, K. J., Sánchez, P., et al. 2021, MNRAS, 507, 5087, doi: 10.1093/mnras/stab2365

Barucci, M. A., Fulchignoni, M., Ji, J., Marchin, S., & Thomas, N. 2015, in Asteroids IV, 433–450, doi: 10.2458/azu_uapress_9780816532131-ch023

Behrend, R. 2005, Optical lightcurves of 99942 Apophis, http://obswww.unige.ch/~behrend/page5cou.html#099942

Benson, C. J., Scheeres, D. J., & Moskovitz, N. A. 2020, Icarus, 340, 113518, doi: 10.1016/j.icarus.2019.113518

Berg, O., Richardson, F., & Burton, H. 1973, NASA SP-330, 16

Bernauer, F., Garcia, R. F., Murdoch, N., et al. 2020, Earth, Planets and Space, doi: 10.1186/s40623-020-01333-9

Beuzit, J. L., Vigan, A., Mouillet, D., et al. 2019, A&A, 631, A155, doi: 10.1051/0004-6361/201935251

Binzel, R. P., A'Hearn, M., Asphaug, E., et al. 2003, Planet. Space Sci., 51, 443, doi: 10.1016/S0032-0633(03)00051-5

Binzel, R. P., Rivkin, A. S., Thomas, C. A., et al. 2009, Icarus, 200, 480, doi: 10.1016/j.icarus.2008.11.028

Binzel, R. P., Morbidelli, A., Merouane, S., et al. 2010, Nature, 463, 331, doi: 10.1038/nature08709

Borisov, G., Devogèle, M., Cellino, A., et al. 2018, MNRAS, 480, L131, doi: 10.1093/mnrasl/sly140

Britt, D. T., Yeomans, D., Housen, K., & Consolmagno, G. 2002, in Asteroids III, 485–500

Brozović, M., Benner, L. A. M., Magri, C., et al. 2010, Icarus, 208, 207, doi: 10.1016/j.icarus.2010.01.035

Brozović, M., Park, R., McMichael, J., et al. 2017, in 2017 International Symposium on Space Technology and Science, International Symposium on Space Technology and Science, 7

Brozović, M., Benner, L. A. M., McMichael, J. G., et al. 2018, Icarus, 300, 115, doi: 10.1016/j.icarus.2017.08.032

Brozović, M., Benner, L. A., Magri, C., et al. 2017, Icarus, 286, 314, doi: https://doi.org/10.1016/j.icarus.2016.10.016

Brozović, M., Benner, L. A., McMichael, J. G., et al. 2018, Icarus, 300, 115, doi: https://doi.org/10.1016/j.icarus.2017.08.032

Buie, M. W., & Keller, J. M. 2016, AJ, 151, 73, doi: 10.3847/0004-6256/151/3/73

Busch, M. W. 2009, Icarus, doi: 10.1016/j.icarus.2008.12.003

—. 2010, PhD thesis, California Institute of Technology

Cambioni, S., de Kleer, K., & Shepard, M. 2022, Journal of Geophysical Research: Planets, doi: 10.1029/2021JE007091

Carter, L. M. 2005, PhD thesis, Cornell University, New York

Cellino, A., Hutton, R. G., Tedesco, E. F., Di Martino, M., & Brunini, A. 1999, Icarus, 138, 129, doi: 10.1006/icar.1998.6062
Chamberlain, M. A., Lovell, A. J., & Sykes, M. V. 2007, Icarus, 192, 448, doi: 10.1016/j.icarus.2007.08.003
Chesley, S. R. 2006, in Asteroids, Comets, Meteors, ed. D. Lazzaro, S. Ferraz-Mello, & J. A. Fernández, Vol. 229, 215–228, doi: 10.1017/S1743921305006769
Chesley, S. R., & Farnocchia, D. 2020, in LPI Contributions, Vol. 2242, Apophis T-9 Years: Knowledge Opportunities for the Science of Planetary Defense, 2049
Chesley, S. R., French, A. S., Davis, A. B., et al. 2020, Journal of Geophysical Research (Planets), 125, e06363, doi: 10.1029/2019JE006363
Clampin, M. 2008, Advances in Space Research, 41, 1983, doi: 10.1016/j.asr.2008.01.010
Clark, C. A., van Belle, G. T., Horch, E. P., et al. 2020, in Society of Photo-Optical Instrumentation Engineers (SPIE) Conference Series, Vol. 11446, Society of Photo-Optical Instrumentation Engineers (SPIE) Conference Series, 114462A, doi: 10.1117/12.2563055
de Kleer, K., Butler, B., Cordiner, M., et al. 2021, Bulletin of the American Astronomical Society, doi: 10.3847/25c2cfeb.5e44dbf2
Delbò, M., Cellino, A., & Tedesco, E. F. 2007, Icarus, 188, 266, doi: 10.1016/j.icarus.2006.12.024
Delbo, M., Walsh, K. J., Matonti, C., et al. 2022, Nature Geoscience, 15, 453, doi: 10.1038/s41561-022-00940-3
DeMartini, J. V., Richardson, D. C., Barnouin, O. S., et al. 2019, Icarus, 328, 93, doi: 10.1016/j.icarus.2019.03.015
DeMartini, J. V., Richardson, D. C., Barnouin, O. S., et al. 2021, in 7th IAA Planetary Defense Conference, 182
Desmars, J., Camargo, J. I. B., Braga-Ribas, F., et al. 2015, A&A, 584, A96, doi: 10.1051/0004-6361/201526498
Devogèle, M., MacLennan, E., Gustafsson, A., et al. 2020, PSJ, 1, 15, doi: 10.3847/PSJ/ab8e45
Dunham, D. W. 1974, Minor Planet Bulletin, 2, 14
Dunham, D. W., Herald, D., Preston, S., et al. 2016, in Asteroids: New Observations, New Models, ed. S. R. Chesley, A. Morbidelli, R. Jedicke, & D. Farnocchia, Vol. 318, 177–180, doi: 10.1017/S1743921315007231
Elliot, J. L. 1979, ARA&A, 17, 445, doi: 10.1146/annurev.aa.17.090179.002305
Farnocchia, D., & Chesley, S. R. 2022, in LPI Contributions, Vol. 2681, LPI Contributions, 2007
Farnocchia, D., Chesley, S. R., Chodas, P. W., et al. 2013, Icarus, 224, 192, doi: 10.1016/j.icarus.2013.02.020
Farnocchia, D., Eggl, S., Chodas, P. W., Giorgini, J. D., & Chesley, S. R. 2019, Celestial Mechanics and Dynamical Astronomy, 131, 36, doi: 10.1007/s10569-019-9914-4
French, J. R., J., & Hulkower, N. D. 1982, Journal of the British Interplanetary Society, 35, 167
Gaia Collaboration, Brown, A. G. A., Vallenari, A., et al. 2016, A&A, 595, A2, doi: 10.1051/0004-6361/201629512
—. 2018, A&A, 616, A1, doi: 10.1051/0004-6361/201833051
—. 2021, A&A, 650, C3, doi: 10.1051/0004-6361/202039657e
Giorgini, J. D., Benner, L. A. M., Ostro, S. J., Nolan, M. C., & Busch, M. W. 2008, Icarus, 193, 1, doi: 10.1016/j.icarus.2007.09.012
Glenar, D. A., Stubbs, T. J., McCoy, J. E., & Vondrak, R. R. 2011, Planetary and Space Science, 59, 1695, doi: https://doi.org/10.1016/j.pss.2010.12.003
Graves, K. J., Minton, D. A., Hirabayashi, M., DeMeo, F. E., & Carry, B. 2018, Icarus, 304, 162, doi: 10.1016/j.icarus.2017.08.025
Harrington, R. S., Giclas, H. L., & Herget, P. 1975, IAUC, 2737, 1

Hartzell, C., Zimmerman, M., & Hergenrother, C. 2022, PSJ, 3, 85, doi: 10.3847/PSJ/ac5629

Haynes, M. S., Elachi, C., Benner, L. A. M., et al. 2022, in LPI Contributions, Vol. 2681, LPI Contributions, 2020

Hickson, D. C., Virkki, A. K., Perillat, P., Nolan, M. C., & Bhiravarasu, S. S. 2021, PSJ, 2, 30, doi: 10.3847/PSJ/abd846

Hirabayashi, M., Kim, Y., & Brozović, M. 2021, Icarus, 365, 114493, doi: https://doi.org/10.1016/j.icarus.2021.114493

Holsapple, K. A., & Michel, P. 2006, Icarus, 183, 331, doi: https://doi.org/10.1016/j.icarus.2006.03.013

Hsu, H.-W., Wang, X., Carroll, A., Hood, N., & Horányi, M. 2022, Nature Astronomy, doi: 10.1038/s41550-022-01717-9

Huang, J., Ji, J., Ye, P., et al. 2013, Scientific Reports, 3, 3411, doi: 10.1038/srep03411

Hudson, R., Ostro, S., & Scheeres, D. 2003, Icarus, 161, 346, doi: https://doi.org/10.1016/S0019-1035(02)00042-8

Hudson, R. S., & Ostro, S. J. 1995, Science, 270, 84, doi: 10.1126/science.270.5233.84

Hudson, S. 1994, Remote Sensing Reviews, 8, 195, doi: 10.1080/02757259309532195

Hunter, T. R., Kneissl, R., Moullet, A., et al. 2015, The Astrophysical Journal, doi: 10.1088/2041-8205/808/1/l2

Jamnejad, V. 2014, An Analysis of High-Power Transmission from DSN Antennas and Aircraft Certification Limits, https://ipnpr.jpl.nasa.gov/progress_report/42-196/196B.pdf

Jawin, E. R., McCoy, T. J., Walsh, K. J., et al. 2022, Icarus, 381, 114992, doi: 10.1016/j.icarus.2022.114992

Landau, L. D., & Lifshitz, E. M. 1976, Mechanics, Third Edition: Volume 1 (Course of Theoretical Physics), 3rd edn. (Butterworth-Heinemann). http://www.worldcat.org/isbn/0750628960

Lauretta, D. S., Hergenrother, C. W., Chesley, S. R., et al. 2019, Science, 366, 3544, doi: 10.1126/science.aay3544

Lee, H. J., Kim, M. J., Marciniak, A., et al. 2022, A&A, 661, L3, doi: 10.1051/0004-6361/202243442

Lee, P. 1996, Icarus, 124, 181, doi: 10.1006/icar.1996.0197

Leith, T. B., Moskovitz, N. A., Mayne, R. G., et al. 2017, Icarus, 295, 61, doi: 10.1016/j.icarus.2017.05.007

Lellouch, E., Moreno, R., Müller, T., et al. 2017, A&A, 608, A45, doi: 10.1051/0004-6361/201731676

Li, J.-Y., Moullet, A., Titus, T. N., H., H. H., & Sykes, M. V. 2020, The Astronomical Journal, doi: 10.3847/1538-3881/ab8305

Licandro, J., Müller, T., Alvarez, C., Alí-Lagoa, V., & Delbo, M. 2016, A&A, 585, A10, doi: 10.1051/0004-6361/201526888

MacLennan, E., Marshall, S., & Granvik, M. 2022, Icarus, 388, 115226, doi: 10.1016/j.icarus.2022.115226

Magri, C., Consolmagno, G. J., Ostro, S. J., Benner, L. A. M., & Beeney, B. R. 2001, M&PS, 36, 1697, doi: 10.1111/j.1945-5100.2001.tb01857.x

Magri, C., Ostro, S. J., Scheeres, D. J., et al. 2007, Icarus, 186, 152, doi: https://doi.org/10.1016/j.icarus.2006.08.004

Mainzer, A., Usui, F., & Trilling, D. E. 2015, in Asteroids IV, 89–106, doi: 10.2458/azu_uapress_9780816532131-ch005

Mainzer, A., Grav, T., Bauer, J., et al. 2011, ApJ, 743, 156, doi: 10.1088/0004-637X/743/2/156

Marchi, S., Barbieri, C., Küppers, M., et al. 2010, Planet. Space Sci., 58, 1116, doi: 10.1016/j.pss.2010.03.017

Margot, J. L., Pravec, P., Taylor, P., Carry, B., & Jacobson, S. 2015, in Asteroids IV, 355–374, doi: 10.2458/azu_uapress_9780816532131-ch019

Masiero, J. R., Mainzer, A. K., & Wright, E. L. 2018, AJ, 156, 62, doi: 10.3847/1538-3881/aacbd4

Masiero, J. R., Wright, E. L., & Mainzer, A. K. 2021, PSJ, 2, 32, doi: 10.3847/PSJ/abda4d

Masiero, J. R., Mainzer, A. K., Bauer, J. M., et al. 2020, PSJ, 1, 5, doi: 10.3847/PSJ/ab7820

Moskovitz, N. A., Benson, C. J., Scheeres, D., et al. 2020, Icarus, 340, 113519, doi: 10.1016/j.icarus.2019.113519

Muinonen, K., Piironen, J., Shkuratov, Y. G., Ovcharenko, A., & Clark, B. E. 2002, in Asteroids III (University of Arizona Press, Tucson), 123–138

Müller, T. G., Kiss, C., Scheirich, P., et al. 2014, A&A, 566, A22, doi: 10.1051/0004-6361/201423841

Nakamura, T., Noguchi, T., Tanaka, M., et al. 2011, Science, 333, 1113, doi: 10.1126/science.1207758

NASA, S. 1998, Radio astronomers find a lost satellite, https://science.nasa.gov/science-news/science-at-nasa/1998/ast28jul98_1

Nugent, C. R., Mainzer, A., Bauer, J., et al. 2016, AJ, 152, 63, doi: 10.3847/0004-6256/152/3/63

Persson, B. N. J., & Biele, J. 2022, Tribology Letters, 70, 34, doi: 10.1007/s11249-022-01570-x

Pravec, P., Scheirich, P., Ďurech, J., et al. 2014, Icarus, 233, 48, doi: 10.1016/j.icarus.2014.01.026

Reddy, V., Sanchez, J. A., Furfaro, R., et al. 2018, The Astronomical Journal, 155, 140, doi: 10.3847/1538-3881/aaaa1c

Reddy, V., Kelley, M. S., Farnocchia, D., et al. 2019, Icarus, 326, 133, doi: 10.1016/j.icarus.2019.02.018

Reddy, V., Kelley, M. S., Dotson, J., et al. 2022a, Icarus, 374, 114790, doi: 10.1016/j.icarus.2021.114790

—. 2022b, PSJ, 3, 123, doi: 10.3847/PSJ/ac66eb

Rennilson, J. J., & Criswell, D. R. 1974, The moon, 10, 121, doi: 10.1007/BF00655715

Rivera-Valentín, E. G., Taylor, P. A., Reddy, V., et al. 2019, in 50th Annual Lunar and Planetary Science Conference, Lunar and Planetary Science Conference, 3016

Rivkin, A. S., Marchis, F., Stansberry, J. A., et al. 2016, PASP, 128, 018003, doi: 10.1088/1538-3873/128/959/018003

Samarasinha, N. H., & Mueller, B. E. A. 2015, Icarus, 248, 347, doi: 10.1016/j.icarus.2014.10.036

Satpathy, A., Mainzer, A., Masiero, J. R., et al. 2022, PSJ, 3, 124, doi: 10.3847/PSJ/ac66d1

Sava, P., & Asphaug, E. 2019, Advances in Space Research, 64, 527, doi: 10.1016/j.asr.2019.04.017

Scheeres, D., Benner, L., Ostro, S., et al. 2005, Icarus, 178, 281, doi: https://doi.org/10.1016/j.icarus.2005.06.002

Scheeres, D. J., Benson, C., Brozović, M., et al. 2020, in LPI Contributions, Vol. 2242, Apophis T-9 Years: Knowledge Opportunities for the Science of Planetary Defense, 2023

Schmid, H. M., Bazzon, A., Roelfsema, R., et al. 2018, A&A, 619, A9, doi: 10.1051/0004-6361/201833620

Schröder, S. E., Keller, H. U., Gutierrez, P., et al. 2010, Planet. Space Sci., 58, 1107, doi: 10.1016/j.pss.2010.04.020

Schröder, S. E., Keller, H. U., Mottola, S., et al. 2015, Planet. Space Sci., 117, 236, doi: 10.1016/j.pss.2015.06.018

Shepard, M. K., de Kleer, K., Cambioni, S., et al. 2021, Planetary Science Journal, doi: 10.3847/PSJ/abfdba

Sheppard, S. S., Fernandez, Y. R., & Moullet, A. 2018, The Astronomical Journal, 156, 270, doi: 10.3847/1538-3881/aae92a

Shoemaker, E. M., & Helin, E. F. 1978, in NASA Conference Publication, Vol. 2053, NASA Conference Publication, ed. D. Morrison & W. C. Wells, 245–256

Simpson, A. M., Brown, M. E., Schemel, M. J., & Butler, B. J. 2022, AJ, 164, 23, doi: 10.3847/1538-3881/ac559e

Takahashi, Y., Busch, M. W., & Scheeres, D. J. 2013, AJ, 146, 95, doi: 10.1088/0004-6256/146/4/95
Taylor, P. A., Rivera-Valentín, E. G., Benner, L. A. M., et al. 2019, Planet. Space Sci., 167, 1, doi: 10.1016/j.pss.2019.01.009
Tholen, D., & Farnocchia, D. 2020, in AAS/Division for Planetary Sciences Meeting Abstracts, Vol. 52, AAS/Division for Planetary Sciences Meeting Abstracts, 214.06
Thomas, C. A., Abell, P., Castillo-Rogez, J., et al. 2016, PASP, 128, 018002, doi: 10.1088/1538-3873/128/959/018002
Trilling, D., van Belle, G., Erasmus, N., et al. 2022, in LPI Contributions, Vol. 2681, LPI Contributions, 2032
Turtle, E. P., Minitti, M. E., Cohen, B. A., et al. 1999, Acta Astronautica, 45, 415, doi: 10.1016/S0094-5765(99)00161-7
Valvano, G., Winter, O. C., Sfair, R., et al. 2022, MNRAS, 510, 95, doi: 10.1093/mnras/stab3299
Vokrouhlický, D., Farnocchia, D., Čapek, D., et al. 2015, Icarus, 252, 277, doi: 10.1016/j.icarus.2015.01.011
Wang, X., Schwan, J., Hsu, H.-W., Grün, E., & Horányi, M. 2016, Geophysical Research Letters, 43, 6103, doi: https://doi.org/10.1002/2016GL069491
Yan, Q., Zhang, X., Xie, L., et al. 2019, Geophysical Research Letters, 46, 9405, doi: https://doi.org/10.1029/2019GL083611
Yu, L.-L., Ji, J., & Ip, W.-H. 2017, Research in Astronomy and Astrophysics, 17, 070, doi: 10.1088/1674-4527/17/7/70
Yu, Y., Richardson, D. C., Michel, P., Schwartz, S. R., & Ballouz, R.-L. 2014, Icarus, 242, 82, doi: 10.1016/j.icarus.2014.07.027
Zimmerman, M. I., Farrell, W. M., Hartzell, C. M., et al. 2016, Journal of Geophysical Research: Planets, 121, 2150, doi: https://doi.org/10.1002/2016JE005049

APPENDIX

A. APOPHIS SPECIFIC ACTION TEAM TERMS OF REFERENCE

National Aeronautics and
Space Administration
Headquarters
Washington, DC 20546-0001

Reply to Attn. of: SMD/Planetary Science Division

TO:	Dr. Bonnie Buratti, Chair, Small Bodies Assessment Group
FROM:	Dr. Lori Glaze, Director, Planetary Science Division
DATE:	March 2, 2022
SUBJECT:	Specific Action Team on the Apophis Earth Close-Approach Science Opportunity: TOR Revision

In reference to the memo of January 7, 2022, requesting that the Small Body Assessment Group (SBAG) convene a Specific Action Team (SAT) to study the Apophis Earth Close Approach Science Opportunity, the Planetary Science Division would like to revise the Terms of Reference (TOR) as indicated by the strikethrough text below. The entire TOR is included for completeness.

TERMS OF REFERENCE

Rationale: Asteroid (99942) Apophis's Earth close approach on April 13, 2029 will be an extremely rare event. Passages of an object this large or larger, this deep or deeper through Earth's gravitational tidal field, are estimated to occur at a mean interval on the order of a thousand years. In principle, the effects of such a tidal encounter on a small body may provide a window into physical properties that would otherwise be inaccessible, Jupiter's 1992 tidal shredding of comet Shoemaker-Levy 9 being a vivid example. However, in terms of the differential tidal stress across the body, the Apophis encounter with Earth will be roughly three orders of magnitude weaker, and the detectable consequences are ambiguous. Thus, it is not fully understood to what extent this rare event offers comparably rare – and *realizable* – science opportunities.

Some such opportunities may be realizable using Earth-based telescopes; others may require a spacecraft in the close vicinity of Apophis. Given this possibility, the fact that Apophis is a potentially hazardous object cannot be overlooked. It has been definitively determined that Apophis will not hit the Earth in 2029, and that it will not pass through any of the keyholes that would lead to an Earth impact later this century. However, while it seems unlikely that an interaction between a spacecraft and the asteroid, intentional or accidental, could move Apophis *into* a keyhole or otherwise increase the risk of a future Earth impact, such a scenario has not yet been decisively ruled out for all possible mission profiles.

Statement of Task: The Specific Action Team (SAT) shall conduct a study to:

1. Identify and quantify the detectable effects on Apophis expected to result from the Earth encounter and identify the measurements and instrumental sensitivities needed to detect them and determine their magnitudes.
2. Assess and prioritize the importance to planetary science and planetary defense of detecting and measuring each of these effects, as well as the value of non-detections (upper limits).
3. Categorize these effects according to (a) detectable using Earth-based assets, (b) detectable using a spacecraft arriving only after Earth close approach, (c) detectable using a spacecraft arriving before Earth close approach; and
4. Quantitatively assess the possibility that spacecraft sent to Apophis could increase the risk of a future Earth impact.

The study shall not:

1. Assess, prioritize, or recommend specific instruments, facilities, flight hardware, mission profiles or concepts.
2. Consider observations or measurements that are not specific to the physical effects of the Earth encounter, unless ~~communication~~ advantages afforded by the close proximity to Earth would enable unique measurements that would otherwise be impossible.

The study shall deliver its report to the NASA Planetary Science Division Director not later than August 15, 2022.

Support: The Center for Near Earth Object Studies (CNEOS) will provide support for item 4 in the Statement of Task, by providing detailed analysis of specific mission profiles to explicitly verify the change in the impact hazard assessment. The SAT may provide CNEOS with a list of example mission parameters for detailed analysis, solely for the purpose of completing item 4, without implying that these represent specific mission concepts. Only missions arriving at Apophis before Earth close approach need detailed analysis.

Membership: The SAT shall be composed of subject matter experts in small-body science, collectively knowledgeable in the areas of geophysics, dynamics, mechanical/material properties, astronomical observations, and flight instrumentation. Following an advertisement of this opportunity to the SBAG membership and consideration of all candidates, the following roster is recommended by the SBAG Steering Committee and concurred by PSD:

- Jessie Dotson*, NASA/Ames Research Center (Chair)
- Marina Brozovic, Jet Propulsion Laboratory
- Steven Chesley, Jet Propulsion Laboratory [Lead for CNEOS support]
- Stephanie Jarmak*, Southwest Research Institute
- Nicholas Moskovitz, Lowell Observatory
- Andrew Rivkin, Johns Hopkins Applied Physics Laboratory
- Paul Sanchez, University of Colorado, Boulder
- Damya Souami, Observatoire de Paris
- Timothy Titus*, US Geological Survey

* denotes members of the SBAG Steering Committee

_____

Dr. Lori S. Glaze
Director Planetary Science Division
NASA Headquarters

cc: Dr. Jessie Dotson, Apophis SAT Chair
Dr. Thomas Statler, PSD, SBAG HQ Liaison
Dr. Stephen Rinehart, PSD, Director, Planetary Research Programs

B. POST-ENCOUNTER OCCULTATION OPPORTUNITIES

This section was completed thanks to exchanges with Josselin Desmars from the ERC Lucky Star team[4], who made the following predictions using NIMA (Numerical Integration of the Motion of an Asteroid) (Desmars et al. 2015) and the *Gaia*-DR3 stellar catalogue (Gaia Collaboration et al. 2021).

We have selected here the best observable events from regions with experienced citizen astronomer observers. Table 5 summarizes the list of these events, their speeds (in km/s), their duration, the geographic region from where they can be observed, as well as the stellar magnitudes.

In Fig. 22, we show the map for a relatively slow event involving an 8.5 mag star. This event (on 2029-10-04) is observable from Western to Eastern Europe. This is one of the earliest relatively easy events that marks the start of a number of more straightforward events. It is followed by a slightly slower occultation of 10.6 mag star, observable across the United States on 2029-10-05 (Fig. 23).

Finally, the last event listed in Table 5 (on 2029-10-12) is a much slower event than the previous ones, of an occultation by a much brighter star (7.9 mag). This event is yet again observable across Europe, and it is one of the very last ones that can presently be predicted, albeit with large uncertainties; however, as optical and radar observations are collected post-encounter, observing this occultation is expected to become feasible.

Table 5. List of some of the best occultation events by Apophis within the months following its April 2029 encounter with Earth.

Date & time (UT)	Location	Star G mag	speed (km/s)	Approx. duration (s)
2029-06-22 09:13:00	Caribbean/Central America	8.7	4.69	0.072 s
2029-07-07 02:52:16	Iberian Peninsula	10.9	6.28	0.054 s
2029-07-14 02:41:31	Western Africa	11.2	6.88	0.049 s
2029-08-07 09:48:56	Northwestern USA	11.1	7.99	0.042 s
2029-08-18 09:01:57	USA and western Mexico	10.9	7.89	0.043 s
2029-09-02 03:17:56	Iberian Peninsula	11.3	7.21	0.047 s
2029-09-15 06:51:02	Canada and USA	11.0	6.03	0.056 s
2029-09-23 06:31:55	Canada and USA	9.8	5.11	0.066 s
2029-09-24 01:30:34	North Africa	8.0	5.01	0.068 s
2029-09-25 10:46:56	USA	11.4	4.83	0.070 s
2029-10-04 01:51:18	Europe (Fig. 22)	8.5	3.60	0.094 s
2029-10-05 09:02:23	USA (Fig. 23)	10.6	3.40	0.1 s
2029-10-08 09:51:23	Mexico	10.7	2.92	0.12 s
2029-10-12 02:12:54	Europe	7.9	2.34	0.14 s

[4] https://lesia.obspm.fr/lucky-star/

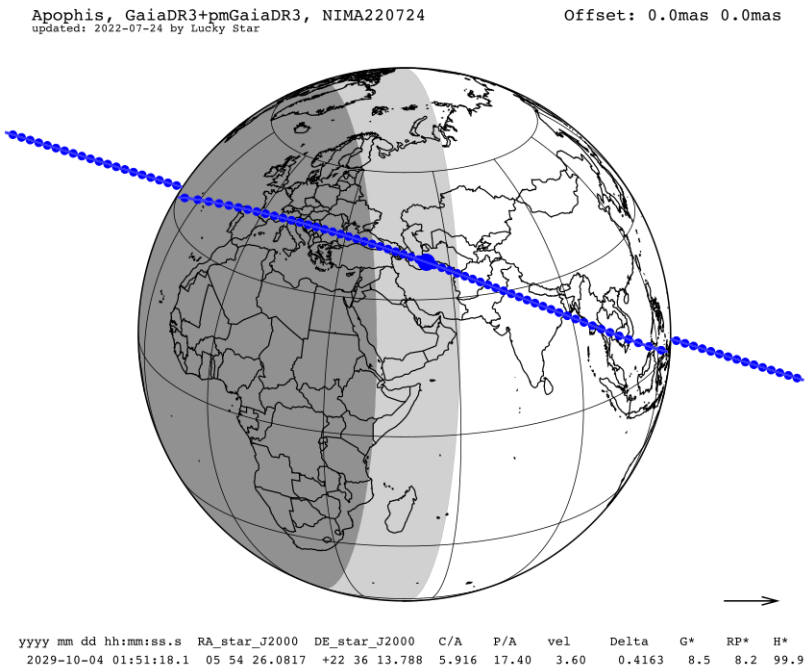

Figure 22. Predicted shadow track for the occultation of an 8.5 G mag star on 2029/10/04, observable across Europe. In this and the following figure, Apophis's shadow is delimited by the continuous blue lines which only show as one continuous line in the figure. The shadow moves from west to east, each blue dot along the track corresponding to one-minute intervals in time. The largest dot corresponds to the geocentric closest approach.

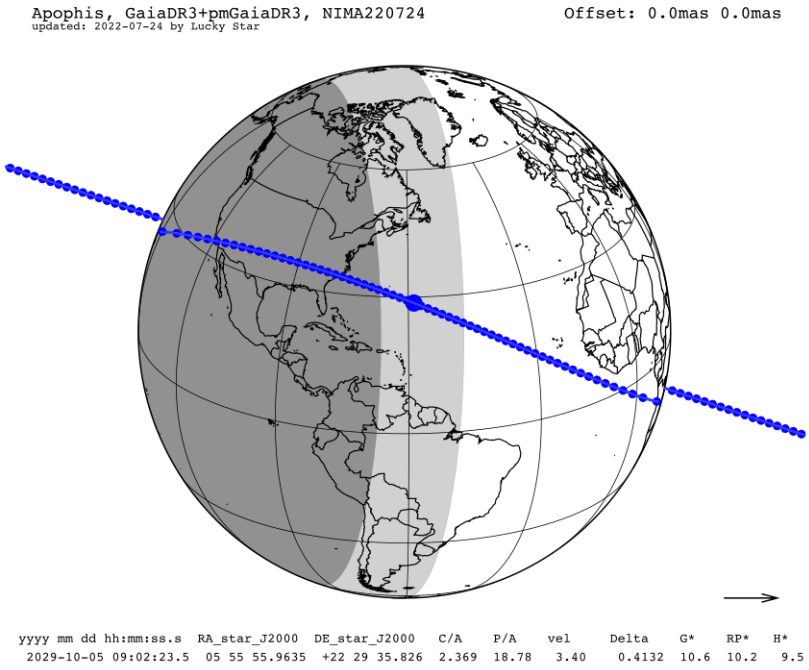

Figure 23. Predicted shadow track for the occultation of a 10.6 G mag star on 2029/10/05, observable across the USA.

We have identified several other events up-to March 2030 and stopped looking into these predictions because of the huge uncertainties, which are larger than 500 mas after March 2030 (Josselin Desmars, private discussion).

Constraints from post-encounter radar data as well as other occultations from the previous opportunities will allow to dramatically reduce these uncertainties for this event and all future events.